DFG Deutsche Forschungsgemeinschaft
Priority Programme 1962

Shape Optimization for Superconductors Governed by H(Curl)-Elliptic Variational Inequalities

Antoine Laurain, Malte Winckler, Irwin Yousept

SPP 1962 | Non-smooth and Complementarity-based Distributed Parameter Systems: Simulation and Hierarchical Optimization

Preprint Number SPP1962-127

received on November 6, 2019

Edited by
SPP1962 at Weierstrass Institute for Applied Analysis and Stochastics (WIAS)
Leibniz Institute in the Forschungsverbund Berlin e.V.
Mohrenstraße 39, 10117 Berlin, Germany
E-Mail: spp1962@wias-berlin.de

World Wide Web: http://spp1962.wias-berlin.de/

SHAPE OPTIMIZATION FOR SUPERCONDUCTORS GOVERNED BY H(CURL)-ELLIPTIC VARIATIONAL INEQUALITIES *

A. LAURAIN†, M. WINCKLER‡, AND I. YOUSEPT‡

Abstract. This paper is devoted to the theoretical and numerical study of an optimal design problem in high-temperature superconductivity (HTS). The shape optimization problem is to find an optimal superconductor shape which minimizes a certain cost functional under a given target on the electric field over a specific domain of interest. For the governing PDE-model, we consider an elliptic curl-curl variational inequality (VI) of the second kind with an L1-type nonlinearity. In particular, the non-smooth VI character and the involved H(curl)-structure make the corresponding shape sensitivity analysis challenging. To tackle the non-smoothness, a penalized dual VI formulation is proposed, leading to the Gâteaux differentiability of the corresponding dual variable mapping. This property allows us to derive the distributed shape derivative of the cost functional through rigorous shape calculus on the basis of the averaged adjoint method. The developed shape derivative turns out to be uniformly stable with respect to the penalization parameter, and strong convergence of the penalized problem is guaranteed. Based on the achieved theoretical findings, we propose 3D numerical solutions, realised using a level set algorithm and a Newton method with the Nédélec edge element discretization. Numerical results indicate a favourable and efficient performance of the proposed approach for a specific HTS application in superconducting shielding.

Key words. shape optimization, high-temperature superconductivity, Maxwell variational inequality, Bean's critical-state model, superconducting shielding, level set method.

AMS subject classifications. 35Q93, 35Q60, 49Q10.

1. Introduction.

The physical phenomenon of superconductivity is characterized by the zero electrical resistance and the expulsion of magnetic fields (Meissner effect) occurring up to a certain level of the operating temperature and magnetic field strength. Nowadays, numerous key technologies can be realised through high-temperature superconductivity (HTS), including magnetic resonance imaging, magnetic levitation, powerful superconducting wires, particle accelerators, magnetic energy storage and many more. In particular, to improve and optimize their efficiency and reliability, advanced shape optimization (design) methods are highly desirable.

For instance, efficiently designed superconducting shields are a practical way to protect certain areas from magnetic fields. Basically, there are only two possible ways for a magnetic field to penetrate an area shielded by a superconductor – through the material itself and through opened parts such as holes or gaps. The former depends solely on the properties of the material, the operating temperature, and the magnetic field strength, whereas the latter is also highly affected by the geometry. In the case of an HTS coil for instance, physical experiments [22] show that the enclosed area is still shielded even if the opened ends are directly facing the field lines. On the other hand, if the diameter gets too large, field lines start penetrating the inside. Thus, the following question arises: how should we design superconducting shields in order to save material and still keep the electromagnetic field penetration to a minimum?

* A. Laurain acknowledges the support of FAPESP, process: 2016/24776-6, and of the Brazilian National Council for Scientific and Technological Development (Conselho Nacional de Desenvolvimento Científico e Tecnológico - CNPq), through the program "Bolsa de Produtividade em Pesquisa - PQ 2015", process: 302493/2015-8. The work of M. Winckler and I. Yousept was supported by the German Research Foundation Priority Program DFG SPP 1962, Project YO 159/2-2.

†Departamento de Matemática Aplicada, Instituto de Matemática e Estatística, Universidade de Ãao Paulo, Rua do Matão, 1010, CEP 05508-090, Ãao Paulo, SP, Brazil, laurain@ime.usp.br.

‡University of Duisburg-Essen, Fakultät für Mathematik, Thea-Leymann-Str. 9, D-45127 Essen, Germany, malte.winckler@uni-due.de, irwin.yousept@uni-due.de.

In the recent past, the Bean critical-state model for HTS has been extensively studied by several authors. In the eddy current case, it leads to a parabolic Maxwell variational inequality (VI) of the first kind (see [4,34]), while in the full Maxwell case it gives rise to a hyperbolic Maxwell VI of the second kind (see [43, 46]). For both parabolic and hyperbolic Maxwell VIs, efficient finite element methods have been proposed and analyzed in [3,10,42].

This paper focuses on the sensitivity analysis and numerical investigation for a shape optimization problem in HTS. Our task is to find an admissible superconductor shape which minimizes a tracking-type objective functional under a given target on the electric field over a specific domain of interest. For the governing PDE-model, we consider the elliptic (time-discrete) counterpart to the Bean critical-state model governed by Maxwell's equations [42,43,46], given by an elliptic **curl-curl** VI of the second kind. To be more precise, let $\Omega \subset \mathbb{R}^3$ be a bounded Lipschitz domain and

$$\mathcal{O} := \{\omega \subset B \,:\, \omega \text{ is open, Lipschitz, with uniform Lipschitz constant } L\},$$

with some subset $B \subset \Omega$. For every admissible superconductor shape $\omega \in \mathcal{O}$, let $\boldsymbol{E} = \boldsymbol{E}(\omega) \in \boldsymbol{H}_0(\mathbf{curl})$ denote the associated electric field given as the solution of

$$(\mathrm{VI}_\omega) \qquad a(\boldsymbol{E}, \boldsymbol{v} - \boldsymbol{E}) + \varphi_\omega(\boldsymbol{v}) - \varphi_\omega(\boldsymbol{E}) \geq \int_\Omega \boldsymbol{f} \cdot (\boldsymbol{v} - \boldsymbol{E})\, dx \quad \forall \boldsymbol{v} \in \boldsymbol{H}_0(\mathbf{curl}),$$

with the elliptic **curl-curl** bilinear form $a\colon \boldsymbol{H}_0(\mathbf{curl}) \times \boldsymbol{H}_0(\mathbf{curl}) \to \mathbb{R}$ defined by

$$a(\boldsymbol{v}, \boldsymbol{w}) := \int_\Omega \nu\, \mathbf{curl}\, \boldsymbol{v} \cdot \mathbf{curl}\, \boldsymbol{w}\, dx + \int_\Omega \varepsilon \boldsymbol{v} \cdot \boldsymbol{w}\, dx,$$

and the non-smooth L^1-type functional $\varphi_\omega\colon \boldsymbol{L}^1(\Omega) \to \mathbb{R}$, $\boldsymbol{v} \mapsto j_c \int_\omega |\boldsymbol{v}(x)|\, dx$. Here, $j_c > 0$ denotes the critical current density of the superconductor ω, and $\epsilon, \nu\colon \Omega \to \mathbb{R}^{3\times 3}$ are the electric permittivity and the magnetic reluctivity, respectively. The right-hand side $\boldsymbol{f}\colon \Omega \to \mathbb{R}^3$ stands for the applied current source. Altogether, the optimal HTS design problem we focus on reads as follows:

$$(\mathrm{P}) \qquad \min_{\omega \in \mathcal{O}} J(\omega) := \frac{1}{2} \int_B \kappa |\boldsymbol{E}(\omega) - \boldsymbol{E}_d|^2\, dx + \int_\omega dx,$$

for some given target $\boldsymbol{E}_d : B \to \mathbb{R}^3$ and weight coefficient $\kappa : B \to (0, \infty)$. The precise mathematical assumptions for all data involved in (P) are specified in Assumption 2.1.

To the best of authors' knowledge, this paper is the first theoretical and numerical study of the shape optimization subject to $\boldsymbol{H}(\mathbf{curl})$-elliptic VI of the second kind. Both the involved $\boldsymbol{H}(\mathbf{curl})$-structure and the non-smooth VI character make the corresponding analysis truly challenging. We refer to [41,44,45] for the optimal control of static Maxwell equations. Quite recently, the optimal control of hyperbolic Maxwell variational inequalities arising in HTS was investigated in [47]. While (P) admits an optimal solution (Theorem 2.4), the differentiability of the dual variable mapping associated with (VI_ω) cannot be guaranteed. This property is however indispensable for our shape sensitivity analysis. Therefore, we propose to approximate (P) by replacing (VI_ω) through its penalized dual formulation (3.1), for which the corresponding dual variable mapping is Gâteaux-differentiable (Lemma 3.1). This allows us to prove our main theoretical result (Theorem 4.5) on the distributed shape derivative of the cost functional through rigorous shape calculus on the basis of the

averaged adjoint method. Importantly, the established shape derivative is uniformly stable with respect to the penalization parameter (Theorem 5.1), and strong convergence of the penalized approach can be guaranteed (Theorem 5.3). In addition, the Newton method is applicable to the penalized dual formulation (3.1). Thus, efficient numerical optimal shapes can be realized by means of a level set algorithm along with the developed shape derivative and a symmetrization strategy. All these theoretical and numerical evidences indicate the favourable performance of our approach to deal with shape optimization problems subject to a VI of the second kind.

Theoretical results on optimal design problems were obtained in [2, 8, 9, 11, 14, 27, 32, 38], but there are few early references for VI-constrained numerical shape optimization (see [13, 21, 30, 37]). Recent publications include [16] regarding a solution algorithm in the infinite dimensional setting for shape optimization problems governed by VIs of the first kind and [12] concerning a shape optimization method based on a regularized variant of VI of the first kind.

The concept of shape derivative [7, 15, 38] is the basis for the sensitivity analysis of shape functionals. We use the *averaged adjoint method* introduced in [39], a Lagrangian-type method for the efficient computation of shape derivatives. Lagrangian methods are commonly used in shape optimization and have the advantage of providing the shape derivative without the need to compute the material derivative of the state (see [1, 5, 7, 17, 18, 20, 33]). Compared to these approaches, the averaged adjoint method is fairly general due to minimal required conditions.

2. Preliminaries. For a given Banach space V, we denote its norm by $\|\cdot\|_V$. If V is a Hilbert space, then $(\cdot,\cdot)_V$ stands for its scalar product and $\|\cdot\|_V$ for the induced norm. In the case of $V=\mathbb{R}^n$, we renounce the subscript in the (Euclidean) norm and write $|\cdot|$. The Euclidean scalar product is denoted by a dot, and $\otimes$ is the standard outer product for vectors in $\mathbb{R}^3$. Hereinafter, a bold typeset indicates vector-valued functions and their respective spaces. The Banach space $\mathcal{C}^1(\Omega,\mathbb{R}^{3\times 3})$ is equipped with the standard norm, and for $\boldsymbol{\mathcal{C}}^{0,1}(\Omega) \coloneqq \mathcal{C}^{0,1}(\Omega,\mathbb{R}^3)$ we use

$$\|\boldsymbol{\theta}\|_{\boldsymbol{\mathcal{C}}^{0,1}(\Omega)} = \sup_{x\in\Omega} |\boldsymbol{\theta}(x)| + \sup_{x\neq y\in\Omega} \frac{|\boldsymbol{\theta}(x)-\boldsymbol{\theta}(y)|}{|x-y|}.$$

Now, we introduce the central Hilbert space used throughout this paper:

$$\boldsymbol{H}(\mathbf{curl}) \coloneqq \{\boldsymbol{v}\in \boldsymbol{L}^2(\Omega) \ : \ \mathbf{curl}\,\boldsymbol{v}\in \boldsymbol{L}^2(\Omega)\},$$

where **curl** is understood in the distributional sense. As usual, $\boldsymbol{\mathcal{C}}_0^\infty(\Omega)$ denotes the space of all infinitely differentiable functions with compact support in Ω. The space $\boldsymbol{H}_0(\mathbf{curl})$ stands for the closure of $\boldsymbol{\mathcal{C}}_0^\infty(\Omega)$ with respect to the $\boldsymbol{H}(\mathbf{curl})$-norm.

Next, we present all the necessary assumptions for the material parameters and the given data in (P) and (VI_ω):

Assumption 2.1 (Material parameters and given data).

(A1) The subset $B\subset\Omega$ is a Lipschitz domain, $\boldsymbol{E}_d\in\boldsymbol{\mathcal{C}}^1(B)$, and $\kappa\in\mathcal{C}^1(B)$.

(A2) We assume $j_c\in\mathbb{R}^+$, and the material parameters $\epsilon,\nu\colon\Omega\to\mathbb{R}^{3\times 3}$ are assumed to be $L^\infty(\Omega,\mathbb{R}^{3\times 3})\cap\mathcal{C}^1(B,\mathbb{R}^{3\times 3})$, symmetric and uniformly positive definite, i.e., there exist $\underline{\nu},\underline{\epsilon}>0$ such that

$$\xi^{\mathsf{T}}\nu(x)\xi \geq \underline{\nu}|\xi|^2 \text{ and } \xi^{\mathsf{T}}\epsilon(x)\xi\geq\underline{\epsilon}|\xi|^2 \quad \text{for a.e. } x\in\Omega \text{ and all } \xi\in\mathbb{R}^3. \tag{2.1}$$

(A3) The right-hand side satisfies $\boldsymbol{f}\in\boldsymbol{L}^2(\Omega)\cap\boldsymbol{\mathcal{C}}^1(B)$.

Remark 2.2.

(i) As pointed out earlier, in the context of superconducting shields, one looks for an optimal superconductor shape ω that minimizes both the electromagnetic field penetration and the volume of material. This can be realised by solving (P) with $\boldsymbol{E}_d = 0$ which obviously satisfies (A1).

(ii) The material assumption (A2) holds true for instance in the case of homogeneous HTS material. In this case, ϵ, μ are constant in B.

(iii) A choice for the $\boldsymbol{f}$ satisfying (A3) is given by an induction coil away from the superconducting region B. In this case, $\boldsymbol{f} \equiv 0$ in B.

For every fixed $\omega \subset \mathcal{O}$ the existence of a unique solution $\boldsymbol{E} \in \boldsymbol{H}_0(\mathbf{curl})$ of (VI_ω) is covered by the classical result [26, Theorem 2.2], since (A2) implies that the bilinear form $a : \boldsymbol{H}_0(\mathbf{curl}) \times \boldsymbol{H}_0(\mathbf{curl}) \to \mathbb{R}$ is coercive and continuous. Additionally, it is well-known (cf. [40]) that there exists a unique $\boldsymbol{\lambda} \in \boldsymbol{L}^\infty(\omega)$ such that

$$\begin{cases} a(\boldsymbol{E}, \boldsymbol{v}) + \displaystyle\int_\omega \boldsymbol{\lambda} \cdot \boldsymbol{v}\, dx = \int_\Omega \boldsymbol{f} \cdot \boldsymbol{v}\, dx \quad \forall \boldsymbol{v} \in \boldsymbol{H}_0(\mathbf{curl}), \\ |\boldsymbol{\lambda}(x)| \le j_c, \quad \boldsymbol{\lambda}(x) \cdot \boldsymbol{E}(x) = j_c |\boldsymbol{E}(x)| \text{ for a.e. } x \in \omega. \end{cases} \tag{2.2}$$

Throughout this paper the following compactness result for the set of domains $\mathcal{O}$ is pivotal to our analysis [15, Theorem 2.4.10].

THEOREM 2.3. *Let Assumption 2.1 hold and $\{\omega_n\}_{n\in\mathbb{N}} \subset \mathcal{O}$. Then, there exist $\omega \in \mathcal{O}$ and a subsequence $\{\omega_{n_k}\}_{k\in\mathbb{N}}$ which converges to ω in the sense of Hausdorff, and in the sense of characteristic functions. Moreover, $\overline{\omega}_{n_k}$ and $\partial\omega_{n_k}$ converge in the sense of Hausdorff towards $\overline{\omega}$ and $\partial\omega$, respectively.*

With Theorem 2.3 at hand, it is possible to prove existence of an optimal shape for (P) directly. However, as the same result is obtained as a byproduct of Theorem 5.3, we do not give a proof at this point.

THEOREM 2.4. *Under Assumption 2.1 the shape optimization problem (P) has an optimal solution $\omega_\star \in \mathcal{O}$.*

3. Penalized shape optimization approach. As pointed out earlier, our shape sensitivity analysis requires the differentiability of the dual variable mapping $\boldsymbol{E} \mapsto \boldsymbol{\lambda}$ in $\boldsymbol{L}^2(\Omega)$, which cannot be guaranteed in general. To cope with this regularity issue, we approximate (P) by

$$\min_{\omega\in\mathcal{O}} J_\gamma(\omega) := \frac{1}{2}\int_B \kappa |\boldsymbol{E}^\gamma(\omega) - \boldsymbol{E}_d|^2 + \int_\omega dx, \tag{P_γ}$$

where $\boldsymbol{E}^\gamma := \boldsymbol{E}^\gamma(\omega) \in \boldsymbol{H}_0(\mathbf{curl})$ is specified by the penalized dual formulation of (2.2):

$$\begin{cases} a(\boldsymbol{E}^\gamma, \boldsymbol{v}) + \displaystyle\int_\omega \boldsymbol{\lambda}^\gamma \cdot \boldsymbol{v}\, dx = \int_\Omega \boldsymbol{f} \cdot \boldsymbol{v}\, dx \quad \forall \boldsymbol{v} \in \boldsymbol{H}_0(\mathbf{curl}) \\ \boldsymbol{\lambda}^\gamma(x) = \dfrac{j_c \gamma \boldsymbol{E}^\gamma(x)}{\max_\gamma\{1, \gamma|\boldsymbol{E}^\gamma(x)|\}} \text{ for a.e. } x \in \omega. \end{cases} \tag{3.1}$$

In this context, $\max_\gamma : \mathbb{R}^3 \to \mathbb{R}$ denotes the Moreau-Yosida type regularization (cf. [6]) of the max-function given by

$$\max_\gamma\{1, x\} := \begin{cases} x & \text{if } x - 1 \ge \frac{1}{2\gamma}, \\ 1 + \frac{\gamma}{2}\left(x - 1 + \frac{1}{2\gamma}\right)^2 & \text{if } |x-1| \le \frac{1}{2\gamma}, \\ 1 & \text{if } x - 1 \le -\frac{1}{2\gamma}. \end{cases} \tag{3.2}$$

The following lemma summarizes the Gâteaux-differentiability result for the dual variable mapping associated with (3.1):

LEMMA 3.1 (Theorem 4.1 in [6]). *Let $\gamma > 0$ and Assumption 2.1 hold. Then,*

$$\boldsymbol{\Lambda}_\gamma \colon \boldsymbol{L}^2(\Omega) \to \boldsymbol{L}^2(\Omega), \quad \boldsymbol{\Lambda}_\gamma(\boldsymbol{e}) \coloneqq \frac{j_c \gamma \boldsymbol{e}}{\max_\gamma\{1, \gamma|\boldsymbol{e}|\}} \tag{3.3}$$

is Gâteaux-differentiable with the Gâteaux-derivative

$$\begin{aligned} \boldsymbol{\Lambda}'_\gamma(\boldsymbol{e})\boldsymbol{w} = {} & \frac{j_c \gamma \boldsymbol{w}}{\max_\gamma\{1, \gamma|\boldsymbol{e}|\}} \\ & - \gamma\left(\mathbb{1}_{\mathcal{A}_\gamma(\boldsymbol{e})} + \gamma\left(\gamma|\boldsymbol{e}| - 1 + \frac{1}{2\gamma}\right)\mathbb{1}_{\mathcal{S}_\gamma(\boldsymbol{e})}\right)\frac{(\boldsymbol{e}\cdot\boldsymbol{w})\boldsymbol{\Lambda}_\gamma(\boldsymbol{e})}{\max_\gamma\{1, \gamma|\boldsymbol{e}|\}|\boldsymbol{e}|} \quad \forall \boldsymbol{e}, \boldsymbol{w} \in \boldsymbol{L}^2(\Omega), \end{aligned} \tag{3.4}$$

where $\mathbb{1}_{\mathcal{A}_\gamma(\boldsymbol{e})}$ and $\mathbb{1}_{\mathcal{S}_\gamma(\boldsymbol{e})}$ stand for the characteristic functions of the disjoint sets $\mathcal{A}_\gamma(\boldsymbol{e}) = \{x \in \Omega : \gamma|\boldsymbol{e}(x)| \geq 1 + 1/2\gamma\}$ and $\mathcal{S}_\gamma(\boldsymbol{e}) = \{x \in \Omega : |\gamma|\boldsymbol{e}(x)| - 1| < 1/2\gamma\}$, respectively. Furthermore, $\boldsymbol{\Lambda}_\gamma$ is Lipschitz-continuous and monotone, i.e.,

$$(\boldsymbol{\Lambda}_\gamma(\boldsymbol{w}_1) - \boldsymbol{\Lambda}_\gamma(\boldsymbol{w}_2), \boldsymbol{w}_1 - \boldsymbol{w}_2)_{\boldsymbol{L}^2(\Omega)} \geq 0 \quad \forall \boldsymbol{w}_1, \boldsymbol{w}_2 \in \boldsymbol{L}^2(\Omega). \tag{3.5}$$

In addition to Lemma 3.1, it is easy to see that the following estimate holds by definition of $\mathcal{S}_\gamma(\boldsymbol{e})$ for every $\boldsymbol{e} \in \boldsymbol{L}^2(\Omega)$:

$$\gamma\left(\gamma|\boldsymbol{e}| - 1 + \frac{1}{2\gamma}\right) \leq 1 \quad \text{a.e. in } \mathcal{S}_\gamma(\boldsymbol{e}). \tag{3.6}$$

For convenience we define the matrix-valued function $\boldsymbol{\psi}^\gamma : \boldsymbol{L}^2(\Omega) \to L^2(\Omega, \mathbb{R}^{3\times 3})$ by

$$\boldsymbol{\psi}^\gamma(\boldsymbol{e}) \coloneqq \frac{j_c \gamma \boldsymbol{I}_3}{\max_\gamma\{1, \gamma|\boldsymbol{e}|\}} - \gamma\left(\mathbb{1}_{\mathcal{A}_\gamma(\boldsymbol{e})} + \gamma\left(\gamma|\boldsymbol{e}| - 1 + \frac{1}{2\gamma}\right)\mathbb{1}_{\mathcal{S}_\gamma(\boldsymbol{e})}\right)\frac{\boldsymbol{e}\otimes\boldsymbol{\Lambda}_\gamma(\boldsymbol{e})}{\max_\gamma\{1, \gamma|\boldsymbol{e}|\}|\boldsymbol{e}|}, \tag{3.7}$$

where $\boldsymbol{I}_3$ denotes the identity matrix in $\mathbb{R}^{3\times 3}$. By multiplying (3.4) with $\boldsymbol{v} \in \boldsymbol{L}^2(\Omega)$ and using $(\boldsymbol{e}\cdot\boldsymbol{w})(\boldsymbol{\Lambda}_\gamma(\boldsymbol{e})\cdot\boldsymbol{v}) = \big(\boldsymbol{e}\otimes\boldsymbol{\Lambda}_\gamma(\boldsymbol{e})\big)\boldsymbol{v}\cdot\boldsymbol{w}$, for all $\boldsymbol{e}, \boldsymbol{v}, \boldsymbol{w} \in \mathbb{R}^3$, we obtain

$$\boldsymbol{\Lambda}'_\gamma(\boldsymbol{e})\boldsymbol{w}\cdot\boldsymbol{v} = \boldsymbol{\psi}^\gamma(\boldsymbol{e})\boldsymbol{v}\cdot\boldsymbol{w} \quad \forall \boldsymbol{e}, \boldsymbol{w}, \boldsymbol{v} \in \boldsymbol{L}^2(\Omega). \tag{3.8}$$

With Lemma 3.1 at hand, the well-posedness of (3.1) follows by the theory of monotone operators [36, p. 40]. Moreover, (3.2) implies for every $\boldsymbol{e} \in \boldsymbol{L}^2(\Omega)$ that

$$\max_\gamma\{1, \gamma|\boldsymbol{e}|\} \geq \gamma|\boldsymbol{e}| \text{ a.e. in } \Omega. \tag{3.9}$$

Applying this estimate to (3.3) yields that

$$\|\boldsymbol{\Lambda}_\gamma(\boldsymbol{e})\|_{\boldsymbol{L}^\infty(\Omega)} \leq j_c \quad \forall \boldsymbol{e} \in \boldsymbol{L}^2(\Omega). \tag{3.10}$$

Obviously, (3.2) yields for every $\boldsymbol{e} \in \boldsymbol{L}^2(\Omega)$ that $\max_\gamma\{1, \gamma|\boldsymbol{e}|\} \geq 1$ almost everywhere in Ω. Hence, we obtain the following estimate for all $\boldsymbol{e}, \boldsymbol{v}, \boldsymbol{w} \in \boldsymbol{L}^2(\Omega)$

$$\begin{aligned} \int_\Omega |\boldsymbol{\psi}^\gamma(\boldsymbol{e})\boldsymbol{v}\cdot\boldsymbol{w}|\,dx &\overbrace{\leq}^{(3.6)} \int_\Omega \frac{j_c\gamma|\boldsymbol{v}\cdot\boldsymbol{w}|}{\max_\gamma\{1,\gamma|\boldsymbol{e}|\}}\,dx + \gamma\int_\Omega \frac{\big|\big(\boldsymbol{e}\otimes\boldsymbol{\Lambda}_\gamma(\boldsymbol{e})\big)\boldsymbol{v}\cdot\boldsymbol{w}\big|}{\max_\gamma\{1,\gamma|\boldsymbol{e}|\}|\boldsymbol{e}|}\,dx \\ &\overbrace{\leq}^{(3.10)} 2j_c\gamma\|\boldsymbol{v}\|_{\boldsymbol{L}^2(\Omega)}\|\boldsymbol{w}\|_{\boldsymbol{L}^2(\Omega)}. \end{aligned} \tag{3.11}$$

The next result states the existence of an optimal solution to (P_γ).

THEOREM 3.2. *Let Assumption 2.1 hold and $\gamma > 0$ be fixed. Then, (P_γ) admits an optimal shape $\omega_\star^\gamma \in \mathcal{O}$.*

Proof. Let $\{\omega_n^\gamma\}_{n\in\mathbb{N}} \subset \mathcal{O}$ be a minimizing sequence for (P_γ) with the corresponding states $\boldsymbol{E}_n^\gamma \in \boldsymbol{H}_0(\mathbf{curl})$ solving (3.1) for $\omega = \omega_n^\gamma$ and $\boldsymbol{\lambda}_n^\gamma := \boldsymbol{\Lambda}(\boldsymbol{E}_n^\gamma)$. Thanks to Theorem 2.3, there exists a subsequence of $\{\omega_n^\gamma\}_{n\in\mathbb{N}}$ (with a slight abuse of notation we use the same index for the subsequence) and $\omega_\star^\gamma \subset \mathcal{O}$ such that $\omega_n^\gamma \to \omega_\star^\gamma$ as $n \to \infty$ in the sense of characteristic functions.

We denote the solution to (3.1) for $\omega = \omega_\star^\gamma$ by $\boldsymbol{E}_\star^\gamma \in \boldsymbol{H}_0(\mathbf{curl})$ and $\boldsymbol{\lambda}_\star^\gamma := \boldsymbol{\Lambda}_\gamma(\boldsymbol{E}_\star^\gamma)$. Now, substracting (3.1) for $\boldsymbol{E}_n^\gamma$ from (3.1) for $\boldsymbol{E}_\star^\gamma$ and testing the resulting equation with $\boldsymbol{v} = \boldsymbol{E}_\star^\gamma - \boldsymbol{E}_n^\gamma$ yields

$$
\begin{aligned}
(3.12)\quad a(\boldsymbol{E}_\star^\gamma - \boldsymbol{E}_n^\gamma, \boldsymbol{E}_\star^\gamma - \boldsymbol{E}_n^\gamma) &= \int_\Omega (\chi_{\omega_\star^\gamma}\boldsymbol{\lambda}_\star^\gamma - \chi_{\omega_n^\gamma}\boldsymbol{\lambda}_n^\gamma)\cdot(\boldsymbol{E}_n^\gamma - \boldsymbol{E}_\star^\gamma)\,dx \\
&= \int_\Omega (\chi_{\omega_\star^\gamma} - \chi_{\omega_n^\gamma})\boldsymbol{\lambda}_n^\gamma\cdot(\boldsymbol{E}_n^\gamma - \boldsymbol{E}_\star^\gamma)\,dx - \underbrace{\int_\Omega \chi_{\omega_\star^\gamma}(\boldsymbol{\lambda}_\star^\gamma - \boldsymbol{\lambda}_n^\gamma)\cdot(\boldsymbol{E}_\star^\gamma - \boldsymbol{E}_n^\gamma)\,dx}_{=(\boldsymbol{\Lambda}_\gamma(\chi_{\omega_\star^\gamma}\boldsymbol{E}_n^\gamma)-\boldsymbol{\Lambda}_\gamma(\chi_{\omega_\star^\gamma}\boldsymbol{E}_\star^\gamma),\chi_{\omega_\star^\gamma}\boldsymbol{E}_n^\gamma-\chi_{\omega_\star^\gamma}\boldsymbol{E}_\star^\gamma)_{\boldsymbol{L}^2(\Omega)}} \\
&\underbrace{\leq}_{(3.5)} \int_\Omega (\chi_{\omega_\star^\gamma} - \chi_{\omega_n^\gamma})\boldsymbol{\lambda}_n^\gamma\cdot(\boldsymbol{E}_n^\gamma - \boldsymbol{E}_\star^\gamma)\,dx.
\end{aligned}
$$

Thus, (3.12) and (A2) of Assumption 2.1 yield

$$
\begin{aligned}
&\min\{\underline{\nu},\underline{\epsilon}\}\|\boldsymbol{E}_\star^\gamma - \boldsymbol{E}_n^\gamma\|_{\boldsymbol{H}(\mathbf{curl})}^2 \leq \|\chi_{\omega_\star^\gamma} - \chi_{\omega_n^\gamma}\|_{L^2(\Omega)}\|\boldsymbol{\lambda}_n^\gamma\|_{\boldsymbol{L}^\infty(\Omega)}\|\boldsymbol{E}_\star^\gamma - \boldsymbol{E}_n^\gamma\|_{\boldsymbol{H}(\mathbf{curl})} \\
&\overset{(3.9)}{\Rightarrow} \quad \|\boldsymbol{E}_\star^\gamma - \boldsymbol{E}_n^\gamma\|_{\boldsymbol{H}(\mathbf{curl})} \leq \frac{j_c}{\min\{\underline{\nu},\underline{\epsilon}\}}\|\chi_{\omega_\star^\gamma} - \chi_{\omega_n^\gamma}\|_{L^2(\Omega)}. \qquad (3.13)
\end{aligned}
$$

This implies $\boldsymbol{E}_n^\gamma \to \boldsymbol{E}_\star^\gamma$ in $\boldsymbol{H}_0(\mathbf{curl})$ since ω_n^γ converges to $\omega_\star^\gamma$ in the sense of characteristic functions as $n \to \infty$. Hence, we obtain

$$
J_\gamma(\omega_n^\gamma) = \frac{1}{2}\int_B \kappa|\boldsymbol{E}_n^\gamma - \boldsymbol{E}_d|^2\,dx + \int_{\omega_n^\gamma} dx \to \frac{1}{2}\int_B \kappa|\boldsymbol{E}_\star^\gamma - \boldsymbol{E}_d|^2\,dx + \int_{\omega_\star^\gamma} dx = J_\gamma(\omega_\star^\gamma).
$$

Finally, the assertion follows since ω_n^γ is a minimizing sequence for (P_γ). ∎

4. Shape sensitivity analysis. This section is devoted to the sensitivity analysis of the shape functional $J_\gamma(\omega)$ in (P_γ) for $\gamma > 0$ fixed. We compute the shape derivative using the averaged adjoint method (see [25,39]). Let $\boldsymbol{T}_t : \Omega \to \Omega$ be the flow of a vector field $\boldsymbol{\theta} \in \boldsymbol{\mathcal{C}}_c^{0,1}(\Omega,\mathbb{R}^3)$ with compact support in B, i.e., $\boldsymbol{T}_t(\boldsymbol{\theta})(X) = x(t,X)$ is the solution to the ordinary differential equation

$$
\frac{\mathrm{d}}{\mathrm{d}t}x(t,X) = \boldsymbol{\theta}(x(t,X)) \quad \text{for } t\in[0,\tau], \quad x(0,X) = X \in \Omega, \qquad (4.1)
$$

for some given $\tau > 0$. It is well-known (see [38, p. 50]) that (4.1) admits a unique solution for a sufficiently small $\tau > 0$. Note that $\boldsymbol{T}_t(B) = B$ and $\boldsymbol{T}_t(X) = X$ for every $X \in \Omega\backslash B$ since $\boldsymbol{\theta}$ has compact support in B. For $\omega \in \mathcal{O}$, we introduce the parameterized family of domains $\omega_t := \boldsymbol{T}_t(\omega)$, for all $t \in [0,\tau]$. Let us now recall the definition of shape derivative used in this paper.

DEFINITION 4.1 (Shape derivative). *Let $K : \mathcal{O} \to \mathbb{R}$ be a shape functional. The Eulerian semiderivative of K at $\omega \in \mathcal{O}$ in direction $\boldsymbol{\theta} \in \boldsymbol{\mathcal{C}}_c^{0,1}(\Omega,\mathbb{R}^3)$ is defined as the*

limit, if it exists,

$$dK(\omega)(\boldsymbol{\theta}) := \lim_{t \searrow 0} \frac{K(\omega_t) - K(\omega)}{t},$$

where $\omega_t = \boldsymbol{T}_t(\omega)$. *Moreover,* K *is said to be shape differentiable at* ω *if it has a Eulerian semiderivative at* ω *for all* $\boldsymbol{\theta} \in \boldsymbol{\mathcal{C}}^{0,1}_c(\Omega, \mathbb{R}^3)$ *and the mapping*

$$dK(\omega) : \boldsymbol{\mathcal{C}}^{0,1}_c(\Omega, \mathbb{R}^3) \to \mathbb{R}, \quad \boldsymbol{\theta} \mapsto dK(\omega)(\boldsymbol{\theta})$$

is linear and continuous. In this case $dK(\omega)(\boldsymbol{\theta})$ *is called the shape derivative at* ω.

In the remainder of this section, we consider the perturbed domain ω_t and denote the corresponding solution of (3.1) for $\omega = \omega_t$ by $\boldsymbol{E}_t^\gamma \in \boldsymbol{H}_0(\mathbf{curl})$.

4.1. Averaged adjoint method. We begin by introducing the Lagrangian $\mathcal{L} : \mathcal{O} \times \boldsymbol{H}_0(\mathbf{curl}) \times \boldsymbol{H}_0(\mathbf{curl}) \to \mathbb{R}$ associated with (P_γ) as follows:

$$\mathcal{L}(\omega, \boldsymbol{e}, \boldsymbol{v}) := \frac{1}{2} \int_B \kappa |\boldsymbol{e} - \boldsymbol{E}_d|^2 \, dx + \int_\omega dx + a(\boldsymbol{e}, \boldsymbol{v}) + \int_\omega \boldsymbol{\Lambda}_\gamma(\boldsymbol{e}) \cdot \boldsymbol{v} \, dx - \int_\Omega \boldsymbol{f} \cdot \boldsymbol{v} \, dx \tag{4.2}$$

where $\boldsymbol{\Lambda}_\gamma$ is given as in (3.3). In view of (4.2), we have for $\omega \in \mathcal{O}$ and $t \in [0, \tau]$ that

$$J_\gamma(\omega_t) = \mathcal{L}(\omega_t, \boldsymbol{E}_t^\gamma, \boldsymbol{v}) \quad \forall \boldsymbol{v} \in \boldsymbol{H}_0(\mathbf{curl}). \tag{4.3}$$

Moreover, as $\mathcal{L}$ is linear in $\boldsymbol{v}$, the problem of finding $\boldsymbol{e} \in \boldsymbol{H}_0(\mathbf{curl})$ such that

$$\partial_{\boldsymbol{v}} \mathcal{L}(\omega_t, \boldsymbol{e}, \boldsymbol{v}; \hat{\boldsymbol{v}}) = a(\boldsymbol{e}, \hat{\boldsymbol{v}}) + \int_{\omega_t} \boldsymbol{\Lambda}_\gamma(\boldsymbol{e}) \cdot \hat{\boldsymbol{v}} \, dx - \int_\Omega \boldsymbol{f} \cdot \hat{\boldsymbol{v}} \, dx = 0 \quad \forall \hat{\boldsymbol{v}} \in \boldsymbol{H}_0(\mathbf{curl})$$

is equivalent to (3.1) with $\omega = \omega_t$ and admits the same unique solution $\boldsymbol{E}_t^\gamma \in \boldsymbol{H}_0(\mathbf{curl})$. In order to pull back the integrals over ω_t to the reference domain ω, one uses the change of variables $x \mapsto \boldsymbol{T}_t(x)$. Furthermore, to avoid the appearance of the composed functions $\boldsymbol{e} \circ \boldsymbol{T}_t$ and $\boldsymbol{v} \circ \boldsymbol{T}_t$ due to this change of variables, we reparameterize the Lagrangian using the following covariant transformation, which is known to be a bijection for $\boldsymbol{H}_0(\mathbf{curl})$ (cf. [29, p. 77]).

$$\Psi_t \colon \boldsymbol{H}_0(\mathbf{curl}) \to \boldsymbol{H}_0(\mathbf{curl}), \qquad \Psi_t(\boldsymbol{e}) := (D\boldsymbol{T}_t^{-\mathsf{T}} \boldsymbol{e}) \circ \boldsymbol{T}_t^{-1}. \tag{4.4}$$

Here $D\boldsymbol{T}_t \colon \mathbb{R}^3 \to \mathbb{R}^{3\times 3}$ stands for the Jacobian matrix function of $\boldsymbol{T}_t$ and we denote $D\boldsymbol{T}_t^{-\mathsf{T}} := \big(D\boldsymbol{T}_t^{-1}\big)^{\mathsf{T}}$. It satisfies the important identity (see [19, Lemma 11])

$$\big(\mathbf{curl}\, \Psi_t(\boldsymbol{e})\big) \circ \boldsymbol{T}_t = \xi(t)^{-1} D\boldsymbol{T}_t \, \mathbf{curl}\, \boldsymbol{e}, \tag{4.5}$$

with $\xi(t) := \det D\boldsymbol{T}_t$. In this paper we always assume $\tau > 0$ small enough such that $\xi(t) > 0$ for every $t \in [0, \tau]$. That is, the transformation $\boldsymbol{T}_t$ preserves orientation. In view of the above discussion, we introduce the *shape-Lagrangian* $G : [0, \tau] \times \boldsymbol{H}_0(\mathbf{curl}) \times \boldsymbol{H}_0(\mathbf{curl}) \to \mathbb{R}$ as

$$\begin{aligned} G(t, \boldsymbol{e}, \boldsymbol{v}) := \mathcal{L}(\omega_t, \Psi_t(\boldsymbol{e}), \Psi_t(\boldsymbol{v})) &= \frac{1}{2} \int_B \kappa |\Psi_t(\boldsymbol{e}) - \boldsymbol{E}_d|^2 \, dx + \int_{\omega_t} dx \\ &+ a(\Psi_t(\boldsymbol{e}), \Psi_t(\boldsymbol{v})) + \int_{\omega_t} \boldsymbol{\Lambda}_\gamma(\Psi_t(\boldsymbol{e})) \cdot \Psi_t(\boldsymbol{v}) \, dx - \int_\Omega \boldsymbol{f} \cdot \Psi_t(\boldsymbol{v}) \, dx. \end{aligned} \tag{4.6}$$

The change of variables $x \mapsto \boldsymbol{T}_t(x)$ inside the integrals (4.4) and (4.5) yields

$$G(t,\boldsymbol{e},\boldsymbol{v}) = \frac{1}{2}\int_B \kappa\circ\boldsymbol{T}_t|D\boldsymbol{T}_t^{-\mathsf{T}}\boldsymbol{e} - \boldsymbol{E}_d\circ\boldsymbol{T}_t|^2\xi(t)\,dx + \int_\omega \xi(t)\,dx + \int_\Omega \mathbb{M}_1(t)\,\mathbf{curl}\,\boldsymbol{e}\cdot$$
$$\mathbf{curl}\,\boldsymbol{v} + \mathbb{M}_2(t)\boldsymbol{e}\cdot\boldsymbol{v}\,dx + \int_\omega \mathbb{M}_3(t,\boldsymbol{e})\cdot\boldsymbol{v}\,dx - \int_\Omega (\boldsymbol{f}\circ\boldsymbol{T}_t)\cdot(D\boldsymbol{T}_t^{-\mathsf{T}}\boldsymbol{v})\xi(t)\,dx, \tag{4.7}$$

with the notations $\mathbb{M}_1(t) := \xi(t)^{-1}D\boldsymbol{T}_t^{\mathsf{T}}(\nu\circ\boldsymbol{T}_t)D\boldsymbol{T}_t$, $\mathbb{M}_2(t) := \xi(t)D\boldsymbol{T}_t^{-1}(\varepsilon\circ\boldsymbol{T}_t)D\boldsymbol{T}_t^{-\mathsf{T}}$ and $\mathbb{M}_3(t,\boldsymbol{e}) := \xi(t)D\boldsymbol{T}_t^{-1}\boldsymbol{\Lambda}_\gamma(D\boldsymbol{T}_t^{-\mathsf{T}}\boldsymbol{e})$. Note that the problem of finding $\boldsymbol{e}_t \in \boldsymbol{H}_0(\mathbf{curl})$ such that $\partial_{\boldsymbol{v}}G(t,\boldsymbol{e}_t,0;\hat{\boldsymbol{v}}) = 0$ for all $\hat{\boldsymbol{v}} \in \boldsymbol{H}_0(\mathbf{curl})$ is equivalent to (3.1) with $\omega = \omega_t$ after applying the change of variables $x \mapsto \boldsymbol{T}_t(x)$. Hence, it has the same unique solution $\boldsymbol{E}_t^\gamma \in \boldsymbol{H}_0(\mathbf{curl})$.

Next, the shape derivative of J_γ is obtained as the partial derivative with respect to t of the shape-Lagrangian G given by (4.7). For the convenience of the reader, we recall the main result of the averaged adjoint method, adapted to our case. A proof can be found in [25, Theorem 2.1] (cf. [39]).

THEOREM 4.2 (Averaged adjoint method). *Let $\gamma > 0$. Moreover, we assume that there exists $\tau \in (0,1]$ such that for every $(t,\boldsymbol{v}) \in [0,\tau]\times\boldsymbol{H}_0(\mathbf{curl})$*

(H1) *the mapping $[0,1] \ni s \mapsto G(t, s\boldsymbol{E}_t^\gamma + (1-s)\boldsymbol{E}_0^\gamma, \boldsymbol{v})$ is absolutely continuous;*

(H2) *the mapping $[0,1] \ni s \mapsto \partial_{\boldsymbol{e}}G(t, s\boldsymbol{E}_t^\gamma + (1-s)\boldsymbol{E}_0^\gamma, \boldsymbol{v};\hat{\boldsymbol{e}})$ belongs to $L^1(0,1)$ for every $\hat{\boldsymbol{e}} \in \boldsymbol{H}_0(\mathbf{curl})$;*

(H3) *there exists a unique $\boldsymbol{P}_t^\gamma \in \boldsymbol{H}_0(\mathbf{curl})$ that solves the averaged adjoint equation*

$$\int_0^1 \partial_{\boldsymbol{e}}G(t, s\boldsymbol{E}_t^\gamma + (1-s)\boldsymbol{E}_0^\gamma, \boldsymbol{P}_t^\gamma;\hat{\boldsymbol{e}})\,ds = 0 \quad \forall\hat{\boldsymbol{e}} \in \boldsymbol{H}_0(\mathbf{curl}); \tag{4.8}$$

(H4) *the family $\{\boldsymbol{P}_t^\gamma\}_{t\in[0,\tau]}$ satisfies*

$$\lim_{t\searrow 0}\frac{G(t,\boldsymbol{E}_0^\gamma,\boldsymbol{P}_t^\gamma) - G(0,\boldsymbol{E}_0^\gamma,\boldsymbol{P}_t^\gamma)}{t} = \partial_t G(0,\boldsymbol{E}_0^\gamma,\boldsymbol{P}_0^\gamma). \tag{4.9}$$

Then, J_γ is shape-differentiable in the sense of Definition 4.1 and it holds that

$$dJ_\gamma(\omega)(\boldsymbol{\theta}) = \frac{d}{dt}J_\gamma(\omega_t)|_{t=0} = \partial_t G(0,\boldsymbol{E}_0^\gamma,\boldsymbol{P}_0^\gamma),$$

where $\boldsymbol{P}_0^\gamma$ is the so-called adjoint state solution of (4.8) with $t = 0$.

We verify that (H1)–(H4) are satisfied so that we may apply Theorem 4.2.

LEMMA 4.3. *Let Assumption 2.1 be satisfied. Then, (H1) and (H2) hold for every $(t,\boldsymbol{v}) \in [0,1]\times\boldsymbol{H}_0(\mathbf{curl})$.*

Proof. First of all, (H1) is a direct consequence of (4.7) and Lemma 3.1. Before we proceed to prove (H2), let us introduce the notation $\mathcal{E}(s) := s\boldsymbol{E}_t^\gamma + (1-s)\boldsymbol{E}_0^\gamma$. Now, fix $\tau \in (0,1]$ and $(t,\boldsymbol{v}) \in [0,\tau]\times\boldsymbol{H}_0(\mathbf{curl})$. Thanks to the Gâteaux-differentiability of $\boldsymbol{\Lambda}_\gamma$ (Lemma 3.1) and using (4.7), we may compute

$$\partial_{\boldsymbol{e}}G(t,\mathcal{E}(s),\boldsymbol{v};\hat{\boldsymbol{e}}) = \int_B \kappa\circ\boldsymbol{T}_t\big(D\boldsymbol{T}_t^{-\mathsf{T}}\hat{\boldsymbol{e}}\cdot(D\boldsymbol{T}_t^{-\mathsf{T}}\mathcal{E}(s) - \boldsymbol{E}_d\circ\boldsymbol{T}_t)\big)\xi(t)\,dx$$
$$+\int_\Omega \mathbb{M}_1(t)\,\mathbf{curl}\,\hat{\boldsymbol{e}}\cdot\mathbf{curl}\,\boldsymbol{v} + \mathbb{M}_2(t)\hat{\boldsymbol{e}}\cdot\boldsymbol{v}\,dx + \int_\omega \partial_{\boldsymbol{e}}\mathbb{M}_3\big(t,\mathcal{E}(s)\big)\hat{\boldsymbol{e}}\cdot\boldsymbol{v}\,dx \tag{4.10}$$

for every $\hat{\boldsymbol{e}} \in \boldsymbol{H}_0(\mathbf{curl})$, where

$$\int_\omega \partial_{\boldsymbol{e}} \mathbb{M}_3\big(t, \mathcal{E}(s)\big)\hat{\boldsymbol{e}} \cdot \boldsymbol{v}\, dx = \int_\omega \xi(t) D\boldsymbol{T}_t^{-1} \boldsymbol{\Lambda}_\gamma'\big(D\boldsymbol{T}_t^{-\mathsf{T}}\mathcal{E}(s)\big)(D\boldsymbol{T}_t^{-\mathsf{T}}\hat{\boldsymbol{e}}) \cdot \boldsymbol{v}\, dx \overset{(3.7)\&(3.8)}{=} \int_\omega \xi(t) D\boldsymbol{T}_t^{-2} \boldsymbol{\psi}^\gamma\big(D\boldsymbol{T}_t^{-\mathsf{T}}\mathcal{E}(s)\big)\boldsymbol{v} \cdot \hat{\boldsymbol{e}}\, dx, \tag{4.11}$$

Moreover, the following asymptotic expansions hold (see [38, Lemma 2.31])

$$\xi(t) = 1 + t\,\mathrm{div}(\boldsymbol{\theta}) + o(t),\ D\boldsymbol{T}_t = \boldsymbol{I}_3 + tD\boldsymbol{\theta} + o(t),\ D\boldsymbol{T}_t^{-1} = \boldsymbol{I}_3 - tD\boldsymbol{\theta} + o(t) \tag{4.12}$$

such that $o(t)/t \to 0$ as $t \to 0$ with respect to $\|\cdot\|_{\mathcal{C}(\Omega)}$ and $\|\cdot\|_{\mathcal{C}(\Omega,\mathbb{R}^{3\times 3})}$, respectively. Hence, (4.12) imply that there exists a constant $C > 0$ only dependent on $\boldsymbol{\theta}$ such that

$$\|\xi(t)\|_{L^\infty(\Omega)} + \|D\boldsymbol{T}_t\|_{L^\infty(\Omega,\mathbb{R}^{3\times 3})} + \|D\boldsymbol{T}_t^{-1}\|_{L^\infty(\Omega,\mathbb{R}^{3\times 3})} \le 1 + C\tau. \tag{4.13}$$

Applying (4.13) in (4.11) leads to

$$\left|\int_\omega \partial_{\boldsymbol{e}} \mathbb{M}_3(t, \mathcal{E}(s))\hat{\boldsymbol{e}} \cdot \boldsymbol{v}\, dx\right| \le (1 + C\tau)^3 \int_\omega \big|\boldsymbol{\psi}^\gamma\big(D\boldsymbol{T}_t^{-\mathsf{T}}\mathcal{E}(s)\big)\boldsymbol{v} \cdot \hat{\boldsymbol{e}}\big|\, dx \overset{(3.11)}{\le} 2j_c\gamma(1 + C\tau)^3 \|\hat{\boldsymbol{e}}\|_{\boldsymbol{L}^2(\Omega)}\|\boldsymbol{v}\|_{\boldsymbol{L}^2(\Omega)} \quad \forall s \in (0,1). \tag{4.14}$$

Thus, the mapping $s \mapsto \int_\omega \partial_{\boldsymbol{e}} \mathbb{M}_3(t, \mathcal{E}(s))\hat{\boldsymbol{e}} \cdot \boldsymbol{v}\, dx$ belongs to $L^\infty(0,1) \subset L^1(0,1)$. In a similar way, since $t \in [0,\tau]$ and $\gamma > 0$ are fixed, (4.13) and (A1) of Assumption 2.1 yield

$$\begin{aligned}
&\int_B \big|\kappa \circ \boldsymbol{T}_t\big(D\boldsymbol{T}_t^{-\mathsf{T}}\hat{\boldsymbol{e}} \cdot D\boldsymbol{T}_t^{-\mathsf{T}}\mathcal{E}(s)\big)\xi(t)\big|\, dx \\
&\quad \le (1 + C\tau)^3 \|\kappa\|_{\mathcal{C}(\Omega)}\|\hat{\boldsymbol{e}}\|_{\boldsymbol{L}^2(\Omega)}\|\mathcal{E}(s)\|_{\boldsymbol{L}^2(\Omega)} \\
&\quad \le (1 + C\tau)^3 \|\kappa\|_{\mathcal{C}(\Omega)}\|\hat{\boldsymbol{e}}\|_{\boldsymbol{L}^2(\Omega)}\big(\|\boldsymbol{E}_0^\gamma\|_{\boldsymbol{L}^2(\Omega)} + s\|\boldsymbol{E}_t^\gamma - \boldsymbol{E}_0^\gamma\|_{\boldsymbol{L}^2(\Omega)}\big) \\
&\quad \le (1 + s)(1 + C\tau)^3 \|\kappa\|_{\mathcal{C}(\Omega)}\|\hat{\boldsymbol{e}}\|_{\boldsymbol{L}^2(\Omega)}\big(\|\boldsymbol{E}_t^\gamma - \boldsymbol{E}_0^\gamma\|_{\boldsymbol{L}^2(\Omega)} + \|\boldsymbol{E}_0^\gamma\|_{\boldsymbol{L}^2(\Omega)}\big).
\end{aligned} \tag{4.15}$$

As the remaining terms in (4.10) are independent of s, (4.14) and (4.15) imply that the mapping $s \mapsto \partial_{\boldsymbol{e}} G(t, \mathcal{E}(s), \boldsymbol{v}; \hat{\boldsymbol{e}})$ belongs to $L^1(0,1)$ for all $\hat{\boldsymbol{e}} \in \boldsymbol{H}_0(\mathbf{curl})$ and $(t, \boldsymbol{v}) \in [0,\tau] \times \boldsymbol{H}_0(\mathbf{curl})$. Thus, the proof is complete. ∎

LEMMA 4.4. *Let Assumption 2.1 hold. Then, there exists $\tau \in (0,1]$ such that (H3) is satisfied for every $t \in [0,\tau]$. Moreover, (H4) holds as well.*

Proof. Fix some arbitrary $\tau > 0$ and denote $\mathcal{E}(s) := s\boldsymbol{E}_t^\gamma + (1-s)\boldsymbol{E}_0^\gamma$ for $s \in (0,1)$. Let $\tau \in (0,1]$ be arbitrarily fixed. In the following, if necessary, we shall reduce $\tau \in (0,1]$ step by step to prove our result. Let $t \in [0,\tau]$ and $\hat{\boldsymbol{e}} \in \boldsymbol{H}_0(\mathbf{curl})$. Thanks to Lemma 4.3, the left-hand side of (4.8) is well-defined, and our goal is to prove the existence of a unique $\boldsymbol{P}_t^\gamma \in \boldsymbol{H}_0(\mathbf{curl})$ satisfying (4.8). In view of (4.10), we note that (4.8) can be written as

$$B_t(\boldsymbol{P}_t^\gamma, \hat{\boldsymbol{e}}) = F_t(\hat{\boldsymbol{e}}) \quad \forall \hat{\boldsymbol{e}} \in \boldsymbol{H}_0(\mathbf{curl}) \tag{4.16}$$

with $B_t\colon \boldsymbol{H}_0(\mathbf{curl}) \times \boldsymbol{H}_0(\mathbf{curl}) \to \mathbb{R}$ and $F_t\colon \boldsymbol{H}_0(\mathbf{curl}) \to \mathbb{R}$ defined by

$$\begin{aligned}
B_t(\boldsymbol{v}, \hat{\boldsymbol{e}}) &:= \int_\Omega \mathbb{M}_1(t)\mathbf{curl}\,\hat{\boldsymbol{e}} \cdot \mathbf{curl}\,\boldsymbol{v} + \mathbb{M}_2(t)\hat{\boldsymbol{e}} \cdot \boldsymbol{v}\, dx + \int_0^1 \int_\omega \partial_{\boldsymbol{e}} \mathbb{M}_3(t, \mathcal{E}(s))\hat{\boldsymbol{e}} \cdot \boldsymbol{v}\, dx\, ds, \\
F_t(\hat{\boldsymbol{e}}) &:= -\int_0^1 \int_B \kappa \circ \boldsymbol{T}_t\big(D\boldsymbol{T}_t^{-\mathsf{T}}\hat{\boldsymbol{e}} \cdot \big(D\boldsymbol{T}_t^{-\mathsf{T}}\mathcal{E}(s) - \boldsymbol{E}_d \circ \boldsymbol{T}_t\big)\big)\xi(t)\, dx\, ds.
\end{aligned}$$

Thanks to (A2) and (4.13) and (4.14), B_t is a bounded bilinear form. In order to apply the Lax-Milgram lemma, we have to prove the coercivity of B_t. The asymptotic expansions (4.12) show that $\mathbb{M}_1(t)$ and $\mathbb{M}_2(t)$ are small perturbations of ν and ϵ, respectively. Thus, if necessary, we may reduce the number $\tau \in (0,1]$ such that, in view of (2.1), $\mathbb{M}_1(t)$ and $\mathbb{M}_2(t)$ are uniformly positive definite for all $t \in [0,\tau]$ with:

$$\int_\Omega \mathbb{M}_1(t)\,\mathbf{curl}\,\boldsymbol{v}\cdot\mathbf{curl}\,\boldsymbol{v} + \mathbb{M}_2(t)\boldsymbol{v}\cdot\boldsymbol{v}\,dx \geq C_1\|\boldsymbol{v}\|^2_{\boldsymbol{H}(\mathbf{curl})} \quad \forall \boldsymbol{v}\in \boldsymbol{H}_0(\mathbf{curl}), \tag{4.17}$$

for some constant $C_1>0$ depending only on $\boldsymbol{\theta}, \epsilon$ and ν. In order to keep the notation short, let us define $\mathcal{K}(s) := D\boldsymbol{T}_t^{-\mathsf{T}}\mathcal{E}(s) \in \boldsymbol{H}_0(\mathbf{curl})$ as well as the sets $\mathcal{A}_\gamma(s) := \mathcal{A}_\gamma(\mathcal{K}(s)) \subset \Omega$ and $\mathcal{S}_\gamma(s) := \mathcal{S}_\gamma(\mathcal{K}(s)) \subset \Omega$ for $s\in(0,1)$ (cf. Lemma 3.1). We estimate the third term in B_t which, in view of (3.7) and (4.11), corresponds to

$$\begin{aligned}\int_0^1\int_\omega \partial_e\mathbb{M}_3(t,\mathcal{E}(s))\boldsymbol{v}\cdot\boldsymbol{v}\,dx\,ds = \int_0^1\int_\omega \xi(t)D\boldsymbol{T}_t^{-2}\Bigg[\frac{j_c\gamma \boldsymbol{I}_3}{\max_\gamma\{1,\gamma|\mathcal{K}(s)|\}}\\ -\gamma\Bigg(\mathbb{1}_{\mathcal{A}_\gamma(s)} + \gamma\Bigg(\gamma|\mathcal{K}(s)| - 1 + \frac{1}{2\gamma}\Bigg)\mathbb{1}_{\mathcal{S}_\gamma(s)}\Bigg)\frac{\mathcal{K}(s)\otimes\boldsymbol{\Lambda}_\gamma(\mathcal{K}(s))}{\max_\gamma\{1,\gamma|\mathcal{K}(s)|\}|\mathcal{K}(s)|}\Bigg]\boldsymbol{v}\cdot\boldsymbol{v}\,dx\,ds.\end{aligned} \tag{4.18}$$

Therefore, we fix $s\in(0,1)$ and estimate the three summands in (4.18) separately. We begin with the first term and note that (4.12) implies, possibly after reducing $\tau>0$, that there exists a constant $C>0$, depending only on $\boldsymbol{\theta}$, such that $\xi(t)\geq 1-C\tau>0$, and $D\boldsymbol{T}_t^{-2}\boldsymbol{\eta}\cdot\boldsymbol{\eta}\geq(1-C\tau)^2|\boldsymbol{\eta}|^2$ for all $\boldsymbol{\eta}\in\mathbb{R}^3$ and almost everywhere in Ω. Hence,

$$\int_\omega j_c\gamma\xi(t)\frac{D\boldsymbol{T}_t^{-2}\boldsymbol{v}\cdot\boldsymbol{v}}{\max_\gamma\{1,\gamma|\mathcal{K}(s)|\}}\,dx \geq (1-C\tau)^3\int_\omega \frac{j_c\gamma|\boldsymbol{v}|^2}{\max_\gamma\{1,\gamma|\mathcal{K}(s)|\}}\,dx. \tag{4.19}$$

Now, we proceed to estimate the integrals over the disjoint sets $\omega\cap\mathcal{A}_\gamma(s)$ and $\omega\cap\mathcal{S}_\gamma(s)$ appearing in the last two summands in (4.18). We obtain

$$\begin{aligned}&\left|\int_{\omega\cap\mathcal{A}_\gamma(s)}\gamma\xi(t)D\boldsymbol{T}_t^{-2}\frac{\mathcal{K}(s)\otimes\boldsymbol{\Lambda}_\gamma(\mathcal{K}(s))\boldsymbol{v}\cdot\boldsymbol{v}}{\max_\gamma\{1,\gamma|\mathcal{K}(s)|\}|\mathcal{K}(s)|}\,dx\right|\\ &\overbrace{\leq}^{(3.3)\&(3.10)} \|\xi(t)\|_{L^\infty(\Omega)}\|D\boldsymbol{T}_t^{-1}\|^2_{L^\infty(\Omega,\mathbb{R}^{3\times3})}\int_{\omega\cap\mathcal{A}_\gamma(s)}\frac{j_c\gamma|\boldsymbol{v}|^2}{\max_\gamma\{1,\gamma|\mathcal{K}(s)|\}}\,dx\\ &\overbrace{\leq}^{(4.13)}(1+C\tau)^3\int_{\omega\cap\mathcal{A}_\gamma(s)}\frac{j_c\gamma|\boldsymbol{v}|^2}{\max_\gamma\{1,\gamma|\mathcal{K}(s)|\}}\,dx.\end{aligned} \tag{4.20}$$

For the last summand, we use the same arguments and also (3.6) to deduce

$$\begin{aligned}&\left|\int_{\omega\cap\mathcal{S}_\gamma(s)}\gamma^2\Bigg(\gamma|\mathcal{K}(s)|-1+\frac{1}{2\gamma}\Bigg)\xi(t)D\boldsymbol{T}_t^{-2}\frac{\mathcal{K}(s)\otimes\boldsymbol{\Lambda}_\gamma(\mathcal{K}(s))\boldsymbol{v}\cdot\boldsymbol{v}}{\max_\gamma\{1,\gamma|\mathcal{K}(s)|\}\,|\mathcal{K}(s)|}\,dx\right|\\ &\qquad\leq(1+C\tau)^3\int_{\omega\cap\mathcal{S}_\gamma(s)}\frac{j_c\gamma|\boldsymbol{v}|^2}{\max_\gamma\{1,\gamma|\mathcal{K}(s)|\}}\,dx.\end{aligned} \tag{4.21}$$

Note that the constant $C>0$ in (4.19)–(4.21) is the same in the three inequalities. Thus, we sum up (4.20) and (4.21) and substract the result from (4.19) to obtain

$$\begin{aligned}\int_\omega \partial_e\mathbb{M}_3(t,\mathcal{E}(s))\boldsymbol{v}\cdot\boldsymbol{v}\,dx \geq \big(1+3(C\tau)^2\big)\int_{\omega\setminus(\mathcal{A}_\gamma(s)\cup\mathcal{S}_\gamma(s))}\frac{j_c\gamma|\boldsymbol{v}|^2}{\max_\gamma\{1,\gamma|\mathcal{K}(s)|\}}\,dx\\ -(6C\tau+2(C\tau)^3)\int_\omega\frac{j_c\gamma|\boldsymbol{v}|^2}{\max_\gamma\{1,\gamma|\mathcal{K}(s)|\}}\,dx.\end{aligned}$$

As the first term is non-negative and $\max_\gamma\{1,\gamma|\mathcal{K}(s)|\} \geq 1$, we conclude for (4.18) that

$$\int_0^1 \int_\omega \partial_e \mathbb{M}_3(t,\mathcal{E}(s))\boldsymbol{v}\cdot\boldsymbol{v}\,dx\,ds \geq -(6C\tau + 2(C\tau)^3) j_c\gamma \|\boldsymbol{v}\|^2_{\boldsymbol{L}^2(\omega)}. \tag{4.22}$$

The coercivity of B_t follows, as (4.17) in combination with (4.22) implies that

$$B_t(\boldsymbol{v},\boldsymbol{v}) \geq \underbrace{(C_1 - 6C\tau - 2(C\tau)^3)}_{=:C_2} \|\boldsymbol{v}\|^2_{\boldsymbol{H}(\mathbf{curl})} \quad \forall \boldsymbol{v}\in \boldsymbol{H}_0(\mathbf{curl}). \tag{4.23}$$

If necessary, we further reduce $\tau \in (0,1]$ such that $C_2 > 0$ holds true. In turn, for all $t\in[0,\tau]$, B_t is coercive with the coercitivity constant $C_2>0$, independent of t. Ultimately, the Lax-Milgram lemma yields the existence of a unique solution $\boldsymbol{P}_t^\gamma \in \boldsymbol{H}_0(\mathbf{curl})$ of the averaged adjoint equation (4.8). Thus, (H3) holds.

We finish this proof by verifying (H4). To this aim, let $\{t_k\}_{k\in\mathbb{N}} \subset (0,\tau]$ be a null sequence. First of all, the sequence $\{\boldsymbol{E}_{t_k}^\gamma\}_{k\in\mathbb{N}} \subset \boldsymbol{H}_0(\mathbf{curl})$ of solutions to the perturbed state equations (3.1) with $\omega = \omega_{t_k}$ is bounded. This follows readily by inserting $\boldsymbol{v} = \boldsymbol{E}_{t_k}^\gamma$ into (3.1) which yields

$$\begin{aligned} \min(\underline{\nu},\underline{\epsilon})\|\boldsymbol{E}_{t_k}^\gamma\|^2_{\boldsymbol{H}(\mathbf{curl})} \leq a(\boldsymbol{E}_{t_k}^\gamma,\boldsymbol{E}_{t_k}^\gamma) &\leq (\|\boldsymbol{f}\|_{\boldsymbol{L}^2(\Omega)} + j_c)\|\boldsymbol{E}_{t_k}^\gamma\|_{\boldsymbol{H}(\mathbf{curl})} \\ \Rightarrow \quad \|\boldsymbol{E}_{t_k}^\gamma\|_{\boldsymbol{H}(\mathbf{curl})} &\leq \min(\underline{\nu},\underline{\epsilon})^{-1}(\|\boldsymbol{f}\|_{\boldsymbol{L}^2(\Omega)} + j_c) \quad \forall k\in\mathbb{N}. \end{aligned} \tag{4.24}$$

Hereafter, we deduce a similar estimate for $\{\boldsymbol{P}_{t_k}^\gamma\}_{k\in\mathbb{N}}$ by testing (4.16) with $\hat{\boldsymbol{e}} = \boldsymbol{P}_{t_k}^\gamma$ and using (4.23) along with (4.13):

$$\begin{aligned} &C_2\|\boldsymbol{P}_{t_k}^\gamma\|^2_{\boldsymbol{H}_0(\mathbf{curl})} \leq B_t(\boldsymbol{P}_{t_k}^\gamma,\boldsymbol{P}_{t_k}^\gamma) = F_t(\boldsymbol{P}_{t_k}^\gamma) \\ &\leq \|\kappa\|_{\mathcal{C}(\Omega)}(1+C\tau)^3(\|\boldsymbol{E}_{t_k}^\gamma\|_{\boldsymbol{L}^2(\Omega)} + \|\boldsymbol{E}_0^\gamma\|_{\boldsymbol{L}^2(\Omega)} + \|\boldsymbol{E}_d\|_{\boldsymbol{L}^2(\Omega)})\|\boldsymbol{P}_{t_k}^\gamma\|_{\boldsymbol{L}^2(\Omega)} \quad \forall k\in\mathbb{N}. \end{aligned} \tag{4.25}$$

Since the constant C_2 and C are independent of $k\in\mathbb{N}$, the above estimate implies the boundedness of $\{\boldsymbol{P}_{t_k}^\gamma\}_{k\in\mathbb{N}} \subset \boldsymbol{H}_0(\mathbf{curl})$. Hence, there exists a subsequence $\{t_{k_j}\}_{j\in\mathbb{N}} \subset \{t_k\}_{k\in\mathbb{N}}$ converging weakly in $\boldsymbol{H}_0(\mathbf{curl})$ to some $\boldsymbol{P}^\star \in \boldsymbol{H}_0(\mathbf{curl})$. By (4.12) and as the solution of (4.16) is unique, passing to the limit $t = t_{k_j} \to 0$ in (4.16) yields $\boldsymbol{P}^\star = \boldsymbol{P}_0^\gamma$. Since $\boldsymbol{P}_0^\gamma$ is independent of the choice of the subsequence $\{t_{k_j}\}_{j\in\mathbb{N}}$, a standard argument implies the weak convergence of the whole sequence:

$$\boldsymbol{P}_{t_k}^\gamma \rightharpoonup \boldsymbol{P}^\star \quad \text{weakly in } \boldsymbol{H}_0(\mathbf{curl}) \quad \text{as } k\to\infty. \tag{4.26}$$

Let us now consider the differential quotient

$$\begin{aligned} \frac{G(t_k,\boldsymbol{E}_0^\gamma,\boldsymbol{P}_{t_k}^\gamma) - G(0,\boldsymbol{E}_0^\gamma,\boldsymbol{P}_{t_k}^\gamma)}{t_k} &= \int_B \frac{\mathbb{M}_0(t_k)-\mathbb{M}_0(0)}{t_k}\,dx + \int_\omega \frac{\xi(t_k)-\xi(0)}{t_k}\,dx \\ &+ \int_\Omega \frac{\mathbb{M}_1(t_k)-\mathbb{M}_1(0)}{t_k}\,\mathbf{curl}\,\boldsymbol{E}_0^\gamma\cdot\mathbf{curl}\,\boldsymbol{P}_{t_k}^\gamma + \frac{\mathbb{M}_2(t_k)-\mathbb{M}_2(0)}{t_k}\boldsymbol{E}_0^\gamma\cdot\boldsymbol{P}_{t_k}^\gamma\,dx \\ &+ \int_\omega \frac{\mathbb{M}_3(t_k,\boldsymbol{E}_0^\gamma)-\mathbb{M}_3(0,\boldsymbol{E}_0^\gamma)}{t_k}\cdot\boldsymbol{P}_{t_k}^\gamma\,dx - \int_\Omega \frac{\mathbb{M}_4(t_k)-\mathbb{M}_4(0)}{t_k}\cdot\boldsymbol{P}_{t_k}^\gamma\,dx, \end{aligned} \tag{4.27}$$

with $\mathbb{M}_0(t_k) := \frac{1}{2}\kappa\circ\boldsymbol{T}_{t_k}|D\boldsymbol{T}_{t_k}^{-\mathsf{T}}\boldsymbol{E}_0^\gamma - \boldsymbol{E}_d\circ\boldsymbol{T}_{t_k}|^2\xi(t_k)$ and $\mathbb{M}_4(t_k) := \xi(t_k)D\boldsymbol{T}_{t_k}^{-1}(\boldsymbol{f}\circ\boldsymbol{T}_{t_k})$. First, (4.12) yields the strong convergence

$$\lim_{k\to\infty}\frac{\xi(t_k)-\xi(0)}{t_k} = \operatorname{div}\boldsymbol{\theta} \quad \text{in } \mathcal{C}(\Omega). \tag{4.28}$$

Moreover, thanks to Assumption 2.1, (4.12) and $\operatorname{supp}\boldsymbol{\theta} \subset\subset B$, we obtain the strong convergence of $\big(\mathbb{M}_i(t_k) - \mathbb{M}_i(0)\big)/t_k$, $i = 0, 1, 2, 4$, as $k \to \infty$ in $L^\infty(\Omega)$:

$$\lim_{k\to\infty} \frac{\mathbb{M}_0(t_k) - \mathbb{M}_0(0)}{t_k} = \frac{1}{2}(\widetilde{\nabla\kappa} \cdot \boldsymbol{\theta} + \kappa \operatorname{div}\boldsymbol{\theta})|\boldsymbol{E}_0^\gamma - \boldsymbol{E}_d|^2 - \kappa(\boldsymbol{E}_0^\gamma - \boldsymbol{E}_d) \cdot (D\boldsymbol{\theta}^\mathsf{T}\boldsymbol{E}_0^\gamma - \widetilde{D\boldsymbol{E}_d}\boldsymbol{\theta}) \tag{4.29}$$

$$\lim_{k\to\infty} \frac{\mathbb{M}_1(t_k) - \mathbb{M}_1(0)}{t_k} = -(\operatorname{div}\boldsymbol{\theta})\nu + D\boldsymbol{\theta}^\mathsf{T}\nu + \nu D\boldsymbol{\theta} + \widetilde{D\nu}\boldsymbol{\theta}, \tag{4.30}$$

$$\lim_{k\to\infty} \frac{\mathbb{M}_2(t_k) - \mathbb{M}_2(0)}{t_k} = (\operatorname{div}\boldsymbol{\theta})\varepsilon - D\boldsymbol{\theta}\varepsilon - \varepsilon D\boldsymbol{\theta}^\mathsf{T} + \widetilde{D\varepsilon}\boldsymbol{\theta}, \tag{4.31}$$

$$\lim_{k\to\infty} \frac{\mathbb{M}_4(t_k) - \mathbb{M}_4(0)}{t_k} = (\operatorname{div}\boldsymbol{\theta})\boldsymbol{f} - D\boldsymbol{\theta}\boldsymbol{f} + \widetilde{D\boldsymbol{f}}\boldsymbol{\theta}. \tag{4.32}$$

Note that $\widetilde{\nabla\kappa}$ denotes the zero extension of $\nabla\kappa_{|B} \in \boldsymbol{\mathcal{C}}(B)$ to Ω. The same notation is used for $\widetilde{D\boldsymbol{E}_d}, \widetilde{D\varepsilon}, \widetilde{D\nu}, \widetilde{D\boldsymbol{f}}$. Similarly, by the Gâteaux-differentiability of $\boldsymbol{\Lambda}_\gamma$ (see Lemma 3.1), (3.8) and (4.26), we deduce that

$$\lim_{k\to\infty} \frac{\mathbb{M}_3(t_k) - \mathbb{M}_3(0)}{t_k} \cdot \boldsymbol{P}_{t_k}^\gamma = \big((\operatorname{div}\boldsymbol{\theta})\boldsymbol{\Lambda}_\gamma(\boldsymbol{E}_0^\gamma) - D\boldsymbol{\theta}\boldsymbol{\Lambda}_\gamma(\boldsymbol{E}_0^\gamma)\big) \cdot \boldsymbol{P}_0^\gamma - \boldsymbol{\psi}^\gamma(\boldsymbol{E}_0^\gamma)\boldsymbol{P}_0^\gamma \cdot (D\boldsymbol{\theta}^\mathsf{T}\boldsymbol{E}_0^\gamma). \tag{4.33}$$

From (4.28)–(4.33) along with the weak convergence (4.26) and $\operatorname{supp}\boldsymbol{\theta} \subset\subset B$, it follows that

$$\begin{aligned}
&\lim_{k\to\infty} \frac{G(t_k, \boldsymbol{E}_0^\gamma, \boldsymbol{P}_{t_k}^\gamma) - G(0, \boldsymbol{E}_0^\gamma, \boldsymbol{P}_{t_k}^\gamma)}{t_k} \\
&= \int_B \frac{1}{2}(\nabla\kappa \cdot \boldsymbol{\theta} + \kappa \operatorname{div}\boldsymbol{\theta})|\boldsymbol{E}_0^\gamma - \boldsymbol{E}_d|^2 - \kappa(\boldsymbol{E}_0^\gamma - \boldsymbol{E}_d) \cdot (D\boldsymbol{\theta}^\mathsf{T}\boldsymbol{E}_0^\gamma + D\boldsymbol{E}_d\boldsymbol{\theta})\, dx \\
&\quad + \int_\omega \operatorname{div}\boldsymbol{\theta}\, dx + \int_B \big(-(\operatorname{div}\boldsymbol{\theta})\nu + D\boldsymbol{\theta}^\mathsf{T}\nu + \nu D\boldsymbol{\theta} + D\nu\boldsymbol{\theta}\big)\operatorname{\mathbf{curl}}\boldsymbol{E}_0^\gamma \cdot \operatorname{\mathbf{curl}}\boldsymbol{P}_0^\gamma\, dx \\
&\quad + \int_B \big((\operatorname{div}\boldsymbol{\theta})\varepsilon - D\boldsymbol{\theta}\varepsilon - \varepsilon D\boldsymbol{\theta}^\mathsf{T} + D\varepsilon\boldsymbol{\theta}\big)\boldsymbol{E}_0^\gamma \cdot \boldsymbol{P}_0^\gamma\, dx \\
&\quad + \int_\omega (\operatorname{div}\boldsymbol{\theta})\boldsymbol{\Lambda}_\gamma(\boldsymbol{E}_0^\gamma) \cdot \boldsymbol{P}_0^\gamma - D\boldsymbol{\theta}\boldsymbol{\Lambda}_\gamma(\boldsymbol{E}_0^\gamma) \cdot \boldsymbol{P}_0^\gamma - \boldsymbol{\psi}^\gamma(\boldsymbol{E}_0^\gamma)\boldsymbol{P}_0^\gamma \cdot (D\boldsymbol{\theta}^\mathsf{T}\boldsymbol{E}_0^\gamma)\, dx \\
&\quad - \int_B (D\boldsymbol{f}\boldsymbol{\theta} + (\operatorname{div}\boldsymbol{\theta})\boldsymbol{f}) \cdot \boldsymbol{P}_0^\gamma - \boldsymbol{f} \cdot D\boldsymbol{\theta}^\mathsf{T}\boldsymbol{P}_0^\gamma\, dx \\
&= \lim_{k\to\infty} \frac{G(t_k, \boldsymbol{E}_0^\gamma, \boldsymbol{P}_0^\gamma) - G(0, \boldsymbol{E}_0^\gamma, \boldsymbol{P}_0^\gamma)}{t_k} = \partial_t G(0, \boldsymbol{E}_0^\gamma, \boldsymbol{P}_0^\gamma).
\end{aligned} \tag{4.34}$$

Thus, (H4) is valid. ∎

It is easy to see that in the case $t = 0$, the solution $\boldsymbol{P}_0^\gamma \in \boldsymbol{H}_0(\mathbf{curl})$ of (4.8) also satisfies the equation

$$\partial_{\boldsymbol{e}}\mathcal{L}(\omega, \boldsymbol{E}_0^\gamma, \boldsymbol{P}_0^\gamma; \hat{\boldsymbol{e}}) = 0 \quad \forall \hat{\boldsymbol{e}} \in \boldsymbol{H}_0(\mathbf{curl}). \tag{4.35}$$

By definition of the Lagrangian (4.2) and by (4.11) we conclude that (4.35) is equivalent to

$$a(\hat{\boldsymbol{e}}, \boldsymbol{P}_0^\gamma) + \int_\omega \boldsymbol{\psi}^\gamma(\boldsymbol{E}_0^\gamma)\boldsymbol{P}_0^\gamma \cdot \hat{\boldsymbol{e}}\, dx = -\int_B \kappa(\boldsymbol{E}_0^\gamma - \boldsymbol{E}_d) \cdot \hat{\boldsymbol{e}}\, dx, \quad \forall \hat{\boldsymbol{e}} \in \boldsymbol{H}_0(\mathbf{curl}). \tag{4.36}$$

We refer to (4.36) as the *adjoint equation* and we write for simplicity $(\boldsymbol{E}^\gamma, \boldsymbol{P}^\gamma) = (\boldsymbol{E}_0^\gamma, \boldsymbol{P}_0^\gamma)$. We now have all the elements at hand to prove the shape differentiability of J_γ and write the distributed expression of the shape derivative of J_γ.

THEOREM 4.5. *Let Assumption 2.1 be satisfied, $\gamma > 0$, $\omega \in \mathcal{O}$ and $\boldsymbol{\theta} \in \boldsymbol{\mathcal{C}}_c^{0,1}(\Omega)$ with a compact support in B. Furthermore, $\boldsymbol{E}^\gamma \in \boldsymbol{H}_0(\mathbf{curl})$ and $\boldsymbol{P}^\gamma \in \boldsymbol{H}_0(\mathbf{curl})$ denote the solutions to (3.1) and (4.36), respectively. Then, the functional J_γ in (P_γ) is shape differentiable with*

$$dJ_\gamma(\omega)(\boldsymbol{\theta}) = \partial_t G(0, \boldsymbol{E}^\gamma, \boldsymbol{P}^\gamma) = \int_B S_1^\gamma : D\boldsymbol{\theta} + \boldsymbol{S}_0^\gamma \cdot \boldsymbol{\theta}\, dx, \tag{4.37}$$

where $S_1^\gamma \in L^1(B, \mathbb{R}^{3\times 3})$ and $\boldsymbol{S}_0^\gamma \in \boldsymbol{L}^1(B)$ are given by

$$\begin{aligned}
S_1^\gamma = &\Big[\frac{\kappa}{2}|\boldsymbol{E}^\gamma - \boldsymbol{E}_d|^2 + \chi_\omega - \nu\, \mathbf{curl}\, \boldsymbol{E}^\gamma \cdot \mathbf{curl}\, \boldsymbol{P}^\gamma + \varepsilon \boldsymbol{E}^\gamma \cdot \boldsymbol{P}^\gamma + \chi_\omega \boldsymbol{\Lambda}_\gamma(\boldsymbol{E}^\gamma) \cdot \boldsymbol{P}^\gamma \\
&- \boldsymbol{f} \cdot \boldsymbol{P}^\gamma\Big] \boldsymbol{I}_3 - \kappa \boldsymbol{E}^\gamma \otimes (\boldsymbol{E}^\gamma - \boldsymbol{E}_d) + \nu\, \mathbf{curl}\, \boldsymbol{E}^\gamma \otimes \mathbf{curl}\, \boldsymbol{P}^\gamma \\
&+ \nu^\mathsf{T}\, \mathbf{curl}\, \boldsymbol{P}^\gamma \otimes \mathbf{curl}\, \boldsymbol{E}^\gamma - \boldsymbol{P}^\gamma \otimes \varepsilon \boldsymbol{E}^\gamma - \boldsymbol{E}^\gamma \otimes \varepsilon^\mathsf{T} \boldsymbol{P}^\gamma + \boldsymbol{P}^\gamma \otimes \boldsymbol{f} \\
&- \chi_\omega \boldsymbol{\Lambda}_\gamma(\boldsymbol{E}^\gamma) \otimes \boldsymbol{P}^\gamma - \boldsymbol{E}^\gamma \otimes \boldsymbol{\psi}^\gamma(\boldsymbol{E}^\gamma) \boldsymbol{P}^\gamma, \\
\boldsymbol{S}_0^\gamma = &\frac{\nabla \kappa}{2}|\boldsymbol{E}^\gamma - \boldsymbol{E}_d|^2 - \kappa D\boldsymbol{E}_d^\mathsf{T}(\boldsymbol{E}^\gamma - \boldsymbol{E}_d) + (D\nu^\mathsf{T}\, \mathbf{curl}\, \boldsymbol{E}^\gamma)\, \mathbf{curl}\, \boldsymbol{P}^\gamma \\
&+ (D\epsilon^\mathsf{T} \boldsymbol{E}^\gamma) \boldsymbol{P}^\gamma - D\boldsymbol{f}^\mathsf{T} \boldsymbol{P}^\gamma.
\end{aligned}$$

Proof. Thanks to Lemmas 4.3 and 4.4, we may apply the averaged adjoint method (see Theorem 4.2). This yields that J_γ is shape-differentiable in the sense of Definition 4.1 and the shape derivative satisfies

$$dJ_\gamma(\omega)(\boldsymbol{\theta}) = \frac{d}{dt} J_\gamma(\omega_t)|_{t=0} = \partial_t G(0, \boldsymbol{E}^\gamma, \boldsymbol{P}^\gamma), \tag{4.38}$$

where $\partial_t G(0, \boldsymbol{E}^\gamma, \boldsymbol{P}^\gamma)$ is given by (4.34). We note that $D\epsilon, D\nu \colon \Omega \to \mathbb{R}^{3\times 3\times 3}$ are third-order tensors, and their transpose $D\epsilon^\mathsf{T}$, $D\nu^\mathsf{T}$ satisfy $(D\epsilon\boldsymbol{\theta})\boldsymbol{E}^\gamma \cdot \boldsymbol{P}^\gamma = (D\epsilon^\mathsf{T}\boldsymbol{E}^\gamma)\boldsymbol{P}^\gamma \cdot \boldsymbol{\theta}$, and $(D\nu\boldsymbol{\theta})\, \mathbf{curl}\, \boldsymbol{E}^\gamma \cdot \mathbf{curl}\, \boldsymbol{P}^\gamma = (D\nu^\mathsf{T}\, \mathbf{curl}\, \boldsymbol{E}^\gamma)\, \mathbf{curl}\, \boldsymbol{P}^\gamma \cdot \boldsymbol{\theta}$; see [35, Proposition 3.1]. Furthermore, for vectors $\boldsymbol{x}, \boldsymbol{y} \in \mathbb{R}^3$ we have the relations $D\boldsymbol{\theta} : (\boldsymbol{x} \otimes \boldsymbol{y}) = \boldsymbol{x} \cdot D\boldsymbol{\theta}\boldsymbol{y} = D\boldsymbol{\theta}^\mathsf{T}\boldsymbol{x} \cdot \boldsymbol{y}$. Applying these to (4.34) and combining it with (4.38), the tensor expression (4.37) for the shape derivative follows. Finally, the fact that $S_1^\gamma \in L^1(B, \mathbb{R}^{3\times 3})$ and $\boldsymbol{S}_0^\gamma \in \boldsymbol{L}^1(B)$ is a straightforward consequence of the regularity of $\boldsymbol{E}^\gamma, \boldsymbol{P}^\gamma$ and of the other functions involved in the expressions of $\boldsymbol{S}_0^\gamma$ and S_1^γ. This completes the proof. ∎

5. Stability and convergence analysis. In this section we analyze the stability of the shape derivative (4.37) with respect to the penalization parameter $\gamma > 0$. Furthermore, the strong convergence of (P_γ) towards (P) as $\gamma \to \infty$ is studied. The latter also implies the existence of an optimal shape for (P) (see Theorem 2.4).

5.1. Stability analysis of the shape derivative.

THEOREM 5.1. *Let $\omega \in \mathcal{O}$ and Assumption 2.1 hold. Then, the following stability estimate holds*

$$|dJ_\gamma(\omega)(\boldsymbol{\theta})| \le C\|\boldsymbol{\theta}\|_{\boldsymbol{\mathcal{C}}^{0,1}(B)} \quad \forall \boldsymbol{\theta} \in \boldsymbol{\mathcal{C}}_c^{0,1}(\Omega),\ \mathrm{supp}\, \boldsymbol{\theta} \subset\subset B, \tag{5.1}$$

with a constant $C = C(j_c, \kappa, \epsilon, \nu, \boldsymbol{f}, \boldsymbol{E}_d, B, \omega)$ independent of γ.

Proof. First of all, the distributed shape derivative from (4.37) yields the estimate

$$|dJ_\gamma(\omega)(\boldsymbol{\theta})| \leq \big(\|S_1^\gamma\|_{L^1(B,\mathbb{R}^{3\times 3})} + \|\boldsymbol{S}_0^\gamma\|_{\boldsymbol{L}^1(B)}\big)\|\boldsymbol{\theta}\|_{\boldsymbol{\mathcal{C}}^{0,1}(B)}. \tag{5.2}$$

In order to derive upper bounds for $\|S_1^\gamma\|_{L^1(B,\mathbb{R}^{3\times 3})}$ and $\|\boldsymbol{S}_0^\gamma\|_{\boldsymbol{L}^1(B)}$, we begin by proving that the families $\{\boldsymbol{E}^\gamma\}_{\gamma>0}$ and $\{\boldsymbol{P}^\gamma\}_{\gamma>0}$ are uniformly bounded in $\boldsymbol{H}_0(\mathbf{curl})$. In view of (4.24), we have

$$\|\boldsymbol{E}^\gamma\|_{\boldsymbol{H}(\mathbf{curl})} \leq \min(\underline{\nu},\underline{\epsilon})^{-1}(\|\boldsymbol{f}\|_{\boldsymbol{L}^2(\Omega)} + j_c) = C_{\boldsymbol{E}}. \tag{5.3}$$

Moreover, we set $t, s = 0$ in (4.11), which yields

$$\int_\omega \partial_{\boldsymbol{e}}\mathbb{M}_3(0,\mathcal{E}(0))(\boldsymbol{P}^\gamma)\cdot\boldsymbol{P}^\gamma\,dx = \int_\omega \boldsymbol{\psi}^\gamma(\boldsymbol{E}^\gamma)\boldsymbol{P}^\gamma\cdot\boldsymbol{P}^\gamma\,dx \geq 0. \tag{5.4}$$

In fact, the non-negativity of (5.4) follows by similar calculations as (4.18)–(4.22) in the special case $t, s, \tau = 0$. As $\boldsymbol{P}^\gamma$ is the unique solution to (4.36), inserting $\hat{\boldsymbol{e}} = \boldsymbol{P}^\gamma$ implies with (A2)

$$\begin{aligned}\min(\underline{\epsilon},\underline{\nu})\|\boldsymbol{P}^\gamma\|^2_{\boldsymbol{H}(\mathbf{curl})} &\leq a(\boldsymbol{P}^\gamma,\boldsymbol{P}^\gamma)\\ &= -\int_B \kappa(\boldsymbol{E}^\gamma - \boldsymbol{E}_d)\cdot\boldsymbol{P}^\gamma\,dx - \int_\omega \boldsymbol{\psi}^\gamma(\boldsymbol{E}^\gamma)\boldsymbol{P}^\gamma\cdot\boldsymbol{P}^\gamma\,dx.\end{aligned}$$

Hence, we obtain a uniform bound for $\boldsymbol{P}^\gamma$ by means of (5.3) and (5.4), i.e.,

$$\|\boldsymbol{P}^\gamma\|_{\boldsymbol{H}(\mathbf{curl})} \leq \|\kappa\|_{\mathcal{C}(\Omega)}\min(\underline{\epsilon},\underline{\nu})^{-1}\big(C_{\boldsymbol{E}} + \|\boldsymbol{E}_d\|_{\boldsymbol{L}^2(B)}\big) = C_{\boldsymbol{P}}. \tag{5.5}$$

With (5.3) and (5.5) we may now estimate both terms in (5.2) separately. Therefore, let us introduce the notation (see Theorem 4.5)

$$S_1^\gamma := \sum_{i=1}^{14}\Theta_i. \tag{5.6}$$

where $\Theta_i \in L^1(B,\mathbb{R}^{3\times 3})$ for every $i \in \{1,\dots,14\}$. Now, Assumption 2.1, (5.3) and (5.5) together with Hölder's and Young's inequalities yield

$$\begin{aligned}&\sum_{i=1}^{6}\|\Theta_i\|_{L^1(B,\mathbb{R}^{3\times 3})}\\ &\leq \int_B \frac{|\kappa|}{2}|\boldsymbol{E}^\gamma - \boldsymbol{E}_d|^2 + \chi_\omega\,dx + \int_B |\nu\,\mathbf{curl}\,\boldsymbol{E}^\gamma\cdot\mathbf{curl}\,\boldsymbol{P}^\gamma| + |\epsilon\boldsymbol{E}^\gamma\cdot\boldsymbol{P}^\gamma|\,dx\\ &\quad + \int_\omega |\boldsymbol{\Lambda}_\gamma(\boldsymbol{E}^\gamma)\cdot\boldsymbol{P}^\gamma|\,dx + \int_B |\boldsymbol{f}\cdot\boldsymbol{P}^\gamma|\,dx\\ &\overbrace{\leq}^{(5.3)\&(5.5)} \|\kappa\|_{\mathcal{C}(B)}\big(C_{\boldsymbol{E}}^2 + \|\boldsymbol{E}_d\|^2_{\boldsymbol{L}^2(B)}\big) + |\omega| + \big(\|\nu\|_{\mathcal{C}(B,\mathbb{R}^{3\times 3})} + \|\epsilon\|_{\mathcal{C}(B,\mathbb{R}^{3\times 3})}\big)C_{\boldsymbol{E}}C_{\boldsymbol{P}}\\ &\quad + (j_c\sqrt{|\omega|} + \|\boldsymbol{f}\|_{\boldsymbol{L}^2(B)})C_{\boldsymbol{P}}\end{aligned} \tag{5.7}$$

For the remaining terms, we use again Assumption 2.1, (5.3) and (5.5) as well as the identity $|\boldsymbol{x}\otimes\boldsymbol{y}| = |\boldsymbol{x}|\cdot|\boldsymbol{y}|$ for all $\boldsymbol{x},\boldsymbol{y}\in\mathbb{R}^3$ to infer

$$\begin{aligned}\sum_{i=7}^{13}\|\Theta_i\|_{L^1(B,\mathbb{R}^{3\times 3})} &\leq \frac{1}{2}\|\kappa\|_{\mathcal{C}(B)}\big(3C_{\boldsymbol{E}}^2 + \|\boldsymbol{E}_d\|^2_{\boldsymbol{L}^2(B)}\big)\\ &\quad + 2(\|\nu\|_{\mathcal{C}(B,\mathbb{R}^{3\times 3})} + \|\epsilon\|_{\mathcal{C}(B,\mathbb{R}^{3\times 3})})C_{\boldsymbol{E}}C_{\boldsymbol{P}} + (\|\boldsymbol{f}\|_{\boldsymbol{L}^2(B)} + j_c\sqrt{|\omega|})C_{\boldsymbol{P}},\end{aligned} \tag{5.8}$$

where we have also used Young's inequality to obtain the first term in (5.8). Moreover, we may estimate the last summand of S_1^γ as follows

$$\|\Theta_{14}\|_{L^1(\Omega,\mathbb{R}^{3\times 3})} = \|\boldsymbol{E}^\gamma \otimes \boldsymbol{\psi}^\gamma(\boldsymbol{E}^\gamma)\boldsymbol{P}^\gamma\|_{L^1(\Omega,\mathbb{R}^{3\times 3})} \leq \int_\omega |\boldsymbol{\psi}^\gamma(\boldsymbol{E}^\gamma)\boldsymbol{P}^\gamma| \cdot |\boldsymbol{E}^\gamma|\,dx \tag{5.9}$$

$$\overset{(3.6)\&(3.7)}{\leq} \int_\omega \left(\frac{j_c\gamma|\boldsymbol{P}^\gamma|}{\max_\gamma\{1,\gamma|\boldsymbol{E}^\gamma|\}} + \frac{\gamma|\boldsymbol{E}^\gamma \otimes \boldsymbol{\Lambda}_\gamma(\boldsymbol{E}^\gamma)| \cdot |\boldsymbol{P}^\gamma|}{\max_\gamma\{1,\gamma|\boldsymbol{E}^\gamma|\}|\boldsymbol{E}^\gamma|} \right) |\boldsymbol{E}^\gamma|\,dx$$

$$\overset{(3.9)}{\leq} \int_\omega 2j_c|\boldsymbol{P}^\gamma|\,dx \leq 2j_c\sqrt{|\omega|}C_{\boldsymbol{P}}.$$

Gathering (5.7)–(5.9) we deduce the final estimate for S_1^γ

$$\begin{aligned}\|S_1^\gamma\|_{L^1(B,\mathbb{R}^{3\times 3})} \leq{}& \frac{1}{2}\|\kappa\|_{\mathcal{C}(B)}\big(5C_{\boldsymbol{E}}^2 + 3\|\boldsymbol{E}_d\|_{\boldsymbol{L}^2(B)}^2\big) + |\omega| \\ &+ 3\big(\|\nu\|_{\mathcal{C}(B,\mathbb{R}^{3\times 3})} + \|\epsilon\|_{\mathcal{C}(B,\mathbb{R}^{3\times 3})}\big)C_{\boldsymbol{E}}C_{\boldsymbol{P}} + \big(2\|\boldsymbol{f}\|_{\boldsymbol{L}^2(B)} + 4j_c\sqrt{|\omega|}\big)C_{\boldsymbol{P}}.\end{aligned} \tag{5.10}$$

Again, (5.3) and (5.5) with Hölder's and Young's inequalities imply for $\boldsymbol{S}_0^\gamma$

$$\begin{aligned}\|\boldsymbol{S}_0^\gamma\|_{\boldsymbol{L}^1(B)} \leq{}& \int_B \frac{1}{2}|\nabla\kappa| \cdot |\boldsymbol{E}^\gamma - \boldsymbol{E}_d|^2 + |\kappa D\boldsymbol{E}_d^\mathsf{T}(\boldsymbol{E}^\gamma - \boldsymbol{E}_d)|\,dx \\ &+ \int_B |D\nu^\mathsf{T}\,\mathbf{curl}\,\boldsymbol{E}^\gamma| \cdot |\,\mathbf{curl}\,\boldsymbol{P}^\gamma| + |D\epsilon^\mathsf{T}\boldsymbol{E}^\gamma| \cdot |\boldsymbol{P}^\gamma| + |D\boldsymbol{f}^\mathsf{T}\boldsymbol{P}^\gamma|\,dx \\ \leq{}& \frac{1}{2}\|\kappa\|_{\mathcal{C}^1(B)}\big(3C_{\boldsymbol{E}}^2 + 5\|\boldsymbol{E}_d\|_{\boldsymbol{H}^1(B)}^2\big) \\ &+ \big(\|\nu\|_{\mathcal{C}^1(B,\mathbb{R}^{3\times 3})} + \|\epsilon\|_{\mathcal{C}^1(B,\mathbb{R}^{3\times 3})}\big)C_{\boldsymbol{P}}C_{\boldsymbol{E}} + \|\boldsymbol{f}\|_{\boldsymbol{H}^1(B)}C_{\boldsymbol{P}}.\end{aligned} \tag{5.11}$$

Finally, we combine (5.2), (5.10), and (5.11) to conclude

$$\begin{aligned}|dJ_\gamma(\omega)(\boldsymbol{\theta})| \leq \Big[& 4\|\kappa\|_{\mathcal{C}^1(B)}\big(C_{\boldsymbol{E}}^2 + \|\boldsymbol{E}_d\|_{\boldsymbol{H}^1(B)}^2\big) + 4\big(\|\nu\|_{\mathcal{C}^1(B,\mathbb{R}^{3\times 3})} + \|\epsilon\|_{\mathcal{C}^1(B,\mathbb{R}^{3\times 3})}\big)C_{\boldsymbol{E}}C_{\boldsymbol{P}} \\ &+ |\omega| + \big(3\|\boldsymbol{f}\|_{\boldsymbol{H}^1(B)} + 4j_c\sqrt{|\omega|}\big)C_{\boldsymbol{P}}\Big]\|\boldsymbol{\theta}\|_{\boldsymbol{\mathcal{C}}^{0,1}(B)} \qquad \square\end{aligned}$$

Hence, the proof is finished.

5.2. Convergence of the regularized shape optimization problem. Our aim is to prove the strong convergence of (P_γ) towards (P). For this purpose, we recall a helpful result which states the strong convergence of the solution to (3.1) for a fixed $\omega \in \mathcal{O}$. A proof can be found in [6, Corollary 4.3]:

LEMMA 5.2. *Let Assumption 2.1 be satisfied and $\omega \in \mathcal{O}$. Moreover, for every $\gamma > 0$, let $(\boldsymbol{E}^\gamma, \boldsymbol{\lambda}^\gamma) \in \boldsymbol{H}_0(\mathbf{curl}) \times \boldsymbol{L}^\infty(\omega)$ denote the solution to (3.1). Then,*

$$(\boldsymbol{E}^\gamma, \boldsymbol{\lambda}^\gamma) \to (\boldsymbol{E}, \boldsymbol{\lambda}) \quad \text{strongly in } \boldsymbol{H}_0(\mathbf{curl}) \times \boldsymbol{H}_0(\mathbf{curl})^* \text{ as } \gamma \to \infty. \tag{5.12}$$

where $(\boldsymbol{E}, \boldsymbol{\lambda}) \in \boldsymbol{H}_0(\mathbf{curl}) \times \boldsymbol{L}^\infty(\omega)$ is the unique solution to (2.2).

Let us point out that in (5.12) we extended the Lagrange multipliers $\boldsymbol{\lambda}^\gamma, \boldsymbol{\lambda}$ by zero as functions in $\boldsymbol{L}^2(\Omega)$, i.e., we set $\boldsymbol{\lambda}^\gamma(x) = 0$ and $\boldsymbol{\lambda}(x) = 0$ for all $x \in \Omega\backslash\omega$. This zero extension shall also be used in the following theorem.

THEOREM 5.3. *Let Assumption 2.1 hold and* $\{\gamma_n\}_{n\in\mathbb{N}} \subset \mathbb{R}^+$ *be such that* $\gamma_n \to \infty$ *as* $n \to \infty$. *Then, there exists a subsequence of* $\{\gamma_n\}_{n\in\mathbb{N}}$, *still denoted by* $\{\gamma_n\}_{n\in\mathbb{N}}$, *such that the sequence of solutions* $\{\omega^{\gamma_n}\}_{n\in\mathbb{N}}$ *of* (P_γ) *with* $\gamma = \gamma_n$ *converges towards an optimal solution* $\omega_\star \subset \mathcal{O}$ *of* (P) *in the sense of Hausdorff and in the sense of characteristic functions.*

Moreover, $\{(\boldsymbol{E}^{\gamma_n}(\omega^{\gamma_n}), \boldsymbol{\lambda}^{\gamma_n}(\omega^{\gamma_n}))\}_{n\in\mathbb{N}}$ *and* $(\boldsymbol{E}(\omega_\star), \boldsymbol{\lambda}(\omega_\star))$ *as the solutions of* (3.1) *for* $\omega = \omega^{\gamma_n}$ *and* (2.2) *for* $\omega = \omega_\star$, *respectively, satisfy*

$$\lim_{\gamma\to\infty} \|\boldsymbol{E}^{\gamma_n}(\omega^{\gamma_n}) - \boldsymbol{E}(\omega_\star)\|_{\boldsymbol{H}(\mathbf{curl})} = 0, \tag{5.13}$$

$$\lim_{\gamma\to\infty} \|\boldsymbol{\lambda}^{\gamma_n}(\omega^{\gamma_n}) - \boldsymbol{\lambda}(\omega_\star)\|_{\boldsymbol{H}_0(\mathbf{curl})^*} = 0, \tag{5.14}$$

where $\boldsymbol{\lambda}^{\gamma_n}(\omega^{\gamma_n})$ (*resp.* $\boldsymbol{\lambda}(\omega_\star)$) *is extended by zero in* $\Omega \setminus \omega^{\gamma_n}$ (*resp. in* $\Omega \setminus \omega_\star$).

Proof. Thanks to Theorem 2.3 and $\gamma_n \to \infty$, there exists $\omega_\star \in \mathcal{O}$ such that, possibly for a subsequence,

$$\omega^{\gamma_n} \to \omega_\star \quad \text{as } n \to \infty \tag{5.15}$$

in the sense of Hausdorff and in the sense of characteristic functions. Furthermore, we have the estimate

$$\begin{aligned}\|\boldsymbol{E}^{\gamma_n}(\omega^{\gamma_n}) - \boldsymbol{E}(\omega_\star)\|_{\boldsymbol{H}(\mathbf{curl})} \le{}& \|\boldsymbol{E}^{\gamma_n}(\omega^{\gamma_n}) - \boldsymbol{E}^{\gamma_n}(\omega_\star)\|_{\boldsymbol{H}(\mathbf{curl})} \\ &+ \|\boldsymbol{E}^{\gamma_n}(\omega_\star) - \boldsymbol{E}(\omega_\star)\|_{\boldsymbol{H}(\mathbf{curl})}.\end{aligned} \tag{5.16}$$

Now, by virtue of Lemma 5.2, the second term on the right-hand side of (5.16) converges to 0 as $n \to \infty$. For the first term we observe (for every $n \in \mathbb{N}$) that the arguments used to derive (3.13) are applicable. Thus, we substract (3.1) for $\boldsymbol{E}^{\gamma_n}(\omega^{\gamma_n})$ and (3.1) for $\boldsymbol{E}^{\gamma_n}(\omega_\star)$ and test the resulting equation with $\boldsymbol{v} = \boldsymbol{E}^{\gamma_n}(\omega_\star) - \boldsymbol{E}^{\gamma_n}(\omega^{\gamma_n})$. Hereafter, analoguously to (3.12), calculations involving (3.5) yield

$$\|\boldsymbol{E}^{\gamma_n}(\omega^{\gamma_n}) - \boldsymbol{E}^{\gamma_n}(\omega_\star)\|_{\boldsymbol{H}(\mathbf{curl})} \le \frac{j_c}{\min\{\underline{\nu}, \underline{\epsilon}\}} \|\chi_{\omega_\star} - \chi_{\omega^{\gamma_n}}\|_{L^2(\Omega)} \quad \forall n \in \mathbb{N}. \tag{5.17}$$

Combining Lemma 5.2 and (5.15)–(5.17) together leads to (5.13).

Furthermore, substracting (2.2) for $\omega = \omega_\star$ and (3.1) for $\omega = \omega^{\gamma_n}$ implies

$$\begin{aligned}\sup_{\boldsymbol{v}\in\boldsymbol{H}_0(\mathbf{curl})} \frac{(\boldsymbol{\lambda}^{\gamma_n}(\omega^{\gamma_n}) - \boldsymbol{\lambda}(\omega_\star), \boldsymbol{v})_{\boldsymbol{L}^2(\Omega)}}{\|\boldsymbol{v}\|_{\boldsymbol{H}(\mathbf{curl})}} &= \sup_{\boldsymbol{v}\in\boldsymbol{H}_0(\mathbf{curl})} \frac{a(\boldsymbol{E}(\omega_\star) - \boldsymbol{E}^{\gamma_n}(\omega^{\gamma_n}), \boldsymbol{v})}{\|\boldsymbol{v}\|_{\boldsymbol{H}(\mathbf{curl})}} \\ \overbrace{\le}^{(A2)} \max\{\|\epsilon\|_{L^\infty(\Omega,\mathbb{R}^{3\times3})}, \|\nu\|_{L^\infty(\Omega,\mathbb{R}^{3\times3})}\} &\|\boldsymbol{E}(\omega_\star) - \boldsymbol{E}^{\gamma_n}(\omega^{\gamma_n})\|_{\boldsymbol{H}(\mathbf{curl})}.\end{aligned} \tag{5.18}$$

Thus, (5.14) follows from (5.13). It remains to verify that $\omega_\star \in \mathcal{O}$ is in fact a minimizer of (P). First of all, we note that, since ω^{γ_n} is a solution of (P_γ) for $\gamma = \gamma_n$, the following estimate holds

$$J_{\gamma_n}(\omega^{\gamma_n}) = \min_{\omega\in\mathcal{O}} J_{\gamma_n}(\omega) \le J_{\gamma_n}(\omega) \quad \forall \omega \in \mathcal{O}. \tag{5.19}$$

Finally, gathering all the previous results, we obtain for every $\omega \in \mathcal{O}$ that

$$\begin{aligned} J(\omega_\star) = \quad & \frac{1}{2}\int_B \kappa|\boldsymbol{E}(\omega_\star) - \boldsymbol{E}_d|^2 dx + \int_{\omega_\star} dx \\ \overset{(5.13)\&(5.15)}{=} \quad & \lim_{n\to\infty} \frac{1}{2}\int_B \kappa|\boldsymbol{E}^{\gamma_n}(\omega^{\gamma_n}) - \boldsymbol{E}_d|^2 dx + \int_{\omega^{\gamma_n}} dx = \lim_{n\to\infty} J_{\gamma_n}(\omega^{\gamma_n}) \\ \overset{(5.19)}{\leq} \quad & \lim_{n\to\infty} J_{\gamma_n}(\omega) = \lim_{n\to\infty} \frac{1}{2}\int_B \kappa|\boldsymbol{E}^{\gamma_n}(\omega) - \boldsymbol{E}_d|^2 dx + \int_{\omega} dx \\ \overset{(5.12)}{=} \quad & \frac{1}{2}\int_B \kappa|\boldsymbol{E}(\omega) - \boldsymbol{E}_d|^2 dx + \int_{\omega} dx = J(\omega). \end{aligned}$$

This shows $J(\omega_\star) \leq J(\omega)$ for every $\omega \in \mathcal{O}$ which yields the assertion. ∎

Remark 5.4. As we have obtained the optimal shape $\omega_\star \in \mathcal{O}$ in (5.15) as the limit of the optimal shapes for (P_γ), Theorem 2.4 follows immediately from Theorem 5.3.

6. Numerical tests. Our algorithm to obtain a numerical approximation for the optimal shape $\omega_\star$ of (P) is based on a variant of the level set method where the distributed shape derivative (Theorem 4.5) is used to obtain a descent direction (see [25]). We refer to [24] for a detailed description of this algorithm including its implementation in a 2D framework. We consider the proposed approach (P_γ) with $\gamma = 7{\cdot}10^4$. The forward problems (3.1) are computed using the Newton method with a finite element discretization based on the first family of Nédélec's edge elements [31] at roughly 2.000.000 DoFs. As announced in the introduction, we apply our algorithm to two problems stemming from high-temperature superconductivity (HTS), also widely known as type-II superconductivity.

We choose $\Omega = [-2,3]^3$ and $B = [0,1]^3$. For simplicity, we take the material parameters $\epsilon = \nu = \boldsymbol{I}_3$ (cf. (A2)). Moreover, $\boldsymbol{f}$ is a circular current

$$\boldsymbol{f}(x,y,z) = \begin{cases} \dfrac{R}{\sqrt{(y-0.5)^2 + (z-0.5)^2}}(0,\ -z+0.5,\ y-0.5) & \text{for } (x,y,z) \in \Omega_p, \\ 0 & \text{for } (x,y,z) \notin \Omega_p, \end{cases}$$

applied to a pipe coil $\Omega_p \subset \Omega$ which is defined by

$$\Omega_p \coloneqq \left\{(x,y,z) \in \Omega \,:\, |z-0.5| \leq 0.5,\ \sqrt{(x-0.5)^2 + (y-0.5)^2} \in [1.2, 1.6]\right\}.$$

The constant $R > 0$ denotes the electrical resistance of Ω_p (here: $R = 10^{-3}$). As $\Omega_p \cap B = \emptyset$, we have $\boldsymbol{f} \equiv 0$ in B and (A3) is satisfied. Without a superconductor in the system, this current would induce an orthogonal magnetic field which admits its highest field strength inside the coil.

We use the distributed expression (4.37) of the shape derivative to obtain a descent direction $\boldsymbol{\Theta}$. More precisely, let $\boldsymbol{V}_h \subset \boldsymbol{H}^1(B) \cap \boldsymbol{\mathcal{C}}^{0,1}(\overline{B})$ be the space of piecewise linear and continuous finite elements on B. Given a positive definite bilinear form $\mathcal{B} : \boldsymbol{V}_h \times \boldsymbol{V}_h \to \mathbb{R}$, the problem is to find $\boldsymbol{\Theta} \in \boldsymbol{V}_h$ such that

$$\mathcal{B}(\boldsymbol{\Theta}, \boldsymbol{\xi}) = -dJ_\gamma(\omega)(\boldsymbol{\xi}) \text{ for all } \boldsymbol{\xi} \in \boldsymbol{V}_h. \tag{6.1}$$

With this choice, the solution $\boldsymbol{\Theta}$ of (6.1) is defined on B and is a descent direction since $dJ_\gamma(\omega)(\boldsymbol{\Theta}) = -\mathcal{B}(\boldsymbol{\Theta}, \boldsymbol{\Theta}) < 0$ if $\boldsymbol{\Theta} \neq 0$. In our algorithm we choose

$$\mathcal{B}(\boldsymbol{\Theta}, \boldsymbol{\xi}) = \int_B \alpha_1 D\boldsymbol{\Theta} : D\boldsymbol{\xi} + \alpha_2 \boldsymbol{\Theta} \cdot \boldsymbol{\xi}\, dx + \alpha_3 \int_{\partial B} (\boldsymbol{\Theta} \cdot \boldsymbol{n})(\boldsymbol{\xi} \cdot \boldsymbol{n})\, ds, \tag{6.2}$$

with $\alpha_1 = 0.5$, $\alpha_2 = 0.5$ and $\alpha_3 = 1.0$. Moreover, the geometry was optimized in the class of shapes with two symmetries with respect to the planes $x = 0.5$ and $y = 0.5$. This is achieved by symmetrizing $\boldsymbol{\Theta}$ with respect to these axis, and it can be shown that the symmetrized vector field is still a descent direction according to the symmetrization technique proposed in Section 6.4.

All codes are written in PYTHON with the open-source finite-element computational software FENICS [28]. We used PARAVIEW to visualize the 3D plots.

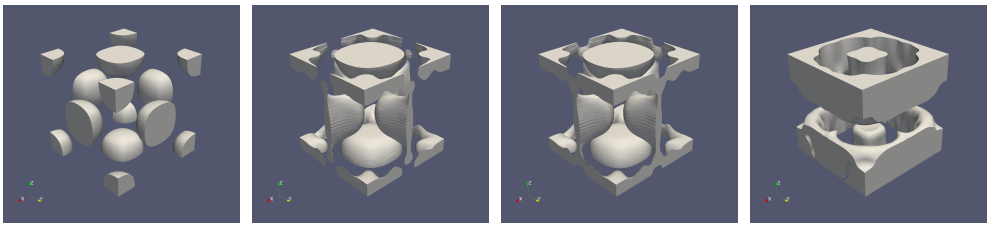

FIG. 1. *Shapes generated by the algorithm at iterations* $0, 42, 45, 143$.

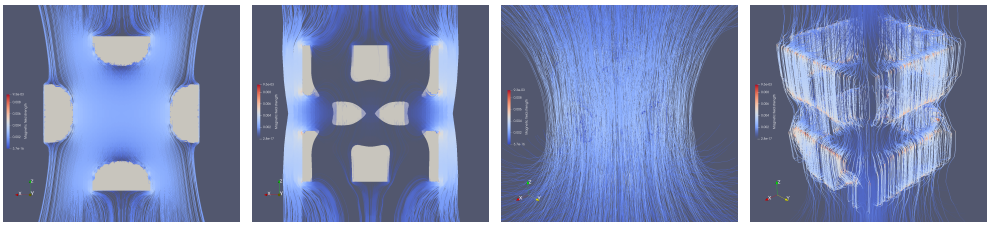

FIG. 2. *Different views on the magnetic field at the initial and the final iteration. a.)–b.): 2D slice in the center. c.)–d.): Total shot from the same view as Figure 1.*

6.1. First example. We set $\boldsymbol{E}_d \equiv 0$ in compliance with (A1) to find the optimal shape of a superconductor that minimizes both the electromagnetic field penetration and the volume of material. This example is motivated by the HTS application in the superconducting shielding (cf. [22]). We take $\kappa \equiv 8 \cdot 10^7$, which is a reasonable choice considering that the electric field strength is roughly $|\boldsymbol{E}| \approx 10^{-3}$ due to the weak applied current strength $|\boldsymbol{f}|$. The initial shape consists of material attached to the boundary of B (see Figure 1a). In Figures 1b to 1d we see some snapshots of the evolving shape generated by our algorithm. The algorithm generates two connected components on the top and the bottom of the (lateral) boundary. It is interesting to observe that the magnetic field ($\mathbf{curl}\, \boldsymbol{E}$) hits the boundary of the bounding box B from above and, despite the small amount of material used, the field lines do not penetrate through the inside of the area enclosed by the superconductor (see Figures 2b and 2d). Moreover, in Figure 2 we can compare the magnetic field penetration for the initial and the final shape from different camera perspectives. The interior of the initial shape is barely protected from penetration, whereas the final shape redirects the magnetic field lines such that they are condensed on the outside of B.

In the final iteration the functional value is around 0.444 at a volume of roughly 0.278 which is only 27.8% of the volume of B. The E-field fraction in the cost functional amounts roughly to 0.166. This means that there is only a weak magnetic field left in small areas of B. The penetration is mostly between the connected components on the lateral surface of the conducting material. The development of the functional

value as well as the volume fraction is documented in Figure 3a and the minimal value is reached after roughly 125 iterations. Thereafter, it remains almost constant.

We also observe a slight increase of the cost functional at iterations 43 and 44, due to a topological change in the design. Indeed, at iteration 42 the components on the lateral sides of the cube are disconnected (see Figure 1b), and then merge at iteration 45 (see Figure 1c). This increase of the cost functional due to a topological change is a well-known issue with the level set method; see [23] for a recent study on this issue. However, in this example the increase in the functional value is negligible and immediately compensated by a sharp decrease.

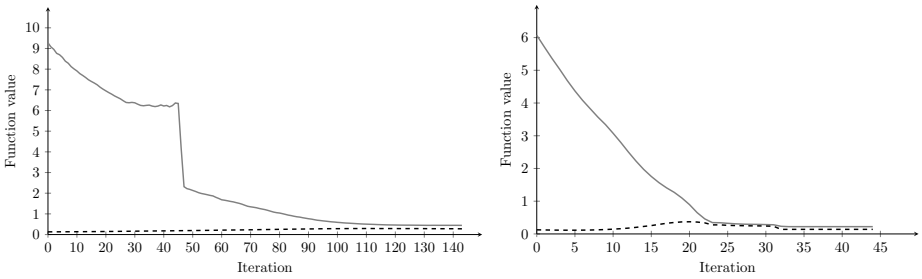

FIG. 3. *Function value (solid) and volume (dashed): 1. Example (left), 2. Example (right).*

6.2. Second example. In our second example, we place a superconducting ball ω_b with radius $r_b = 0.5$ inside B (see Figure 4a) and compute $\boldsymbol{E}_d$ as the corresponding solution of (3.1). The resulting magnetic field is displayed in Figures 5a and 5c. We initialized the algorithm with the same parameters and the same initial shape as in the first example (see Figure 1a). In the end, we obtain two bell-shaped components connected by small transitions on the boundary. In Figures 4b to 4d we see this shape from different camera positions. It corresponds to a functional value of 0.223 where the electric field costs get as low as 0.071 at a volume fraction of 0.153. As the original superconductor was a ball with radius 0.5, our algorithm computed an optimal shape with around 70% less material. The development of the functional value and the volume is documented in Figure 3b. Moreover, the descent in this example is smoother and notably faster than the first example. We explain this by the fact that the second choice of $\boldsymbol{E}_d$ gives more structure than simply $\boldsymbol{E}_d \equiv 0$. Thus, the algorithm has less possibilities to design the superconductor and converges faster.

6.3. Convergence tests with respect to γ. Let us now report on a numerical test to verify our theoretical convergence result (Theorem 5.3). Since no analytical solution is available for the limit case (P), we compare the numerical results of our algorithm with two different regularization parameters $\hat{\gamma} = 7 \cdot 10^4$ and $\tilde{\gamma} = 7 \cdot 10^5$. For these choices, we terminated our algorithm after 143 iterations and computed the norm distance between the two numerical solutions:

$$\|\chi_{\omega^{\hat{\gamma}}} - \chi_{\omega^{\tilde{\gamma}}}\|_{L^1(\Omega)} \approx 2.88 \cdot 10^{-3} \quad \text{and} \quad \|\boldsymbol{E}^{\hat{\gamma}} - \boldsymbol{E}^{\tilde{\gamma}}\|_{\boldsymbol{H}(\mathbf{curl})} \approx 1.39 \cdot 10^{-4}.$$

This relatively small value indicates the convergence for $\gamma \to \infty$ (Theorem 5.3). In particular, we observe that, for sufficiently large penalization parameter γ, a remarkable change in γ would only lead to a small change in the computed optimal shape.

6.4. Shape optimization with symmetric design. In many applications, it is desirable to obtain an optimal design which has certain prescribed symmetries. These can be, for instance, the consequence of symmetries of the geometry and the

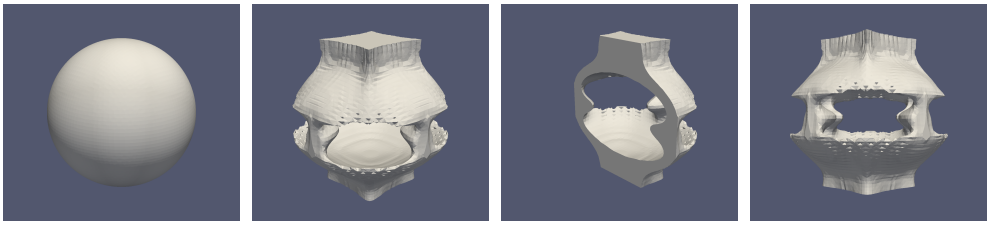

FIG. 4. *The original superconductor and the final shape generated by the algorithm in the second example. The third figure is the final shape clipped along the plane* $x = 0.5$.

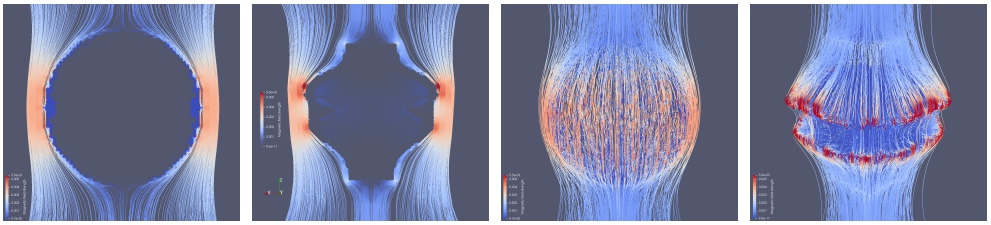

FIG. 5. *Different views on the magnetic field of the original and the final superconductor. Left: 2D slice in the center. Right: Total shot from the same view as Figures 4a and 4b.*

data that imply symmetries in the continuous solution. However, in practice, the numerically optimized design may deviate substantially from these symmetries, usually due to a non-symmetric discretization. This can be mitigated by refining the discretization which may not always be an affordable option, especially for 3D problems. Thus, imposing the symmetry as a constraint for the discretized problem can be a valuable alternative.

In this section we describe a method to obtain a descent direction for our minimization algorithm for (P_γ) while imposing a symmetry constraint. Therefore, we assume $B \subset \mathbb{R}^3$ (cf. (A1)) to be additionally symmetric with respect to some plane $Q \subset \mathbb{R}^3$. Without loss of generality, we may assume that $Q = \{x \in \mathbb{R}^3 \,|\, x_3 = 0\}$. Thanks to Theorem 4.5, the shape derivative of $J_\gamma(\omega)$ exists for every $\omega \in \mathcal{O}$ and admits the following tensor expression (see (4.37))

$$dJ_\gamma(\omega)(\boldsymbol{\theta}) = \int_B S_1 : D\boldsymbol{\theta} + \boldsymbol{S}_0 \cdot \boldsymbol{\theta}\, dx \quad \forall \boldsymbol{\theta} \in \boldsymbol{\mathcal{C}}_c^{0,1}(\Omega) \text{ with } \operatorname{supp} \boldsymbol{\theta} \subset\subset B.$$

Now, a descent direction for J_γ can be found by computing a solution $\widehat{\boldsymbol{\theta}} \in \boldsymbol{V}_h$ of

$$\mathcal{B}(\widehat{\boldsymbol{\theta}}, \boldsymbol{\zeta}) = -dJ_\gamma(\omega)(\boldsymbol{\zeta}) = -\int_B S_1 : D\boldsymbol{\zeta} + \boldsymbol{S}_0 \cdot \boldsymbol{\zeta}\, dx, \quad \forall \boldsymbol{\zeta} \in \boldsymbol{V}_h,$$

where $\mathcal{B}$ is a positive definite bilinear form on $\boldsymbol{V}_h \times \boldsymbol{V}_h$ (see (6.1)). The descent direction $\widehat{\boldsymbol{\theta}} \neq 0$ is not necessarily symmetric with respect to Q. Our aim now is to construct a symmetric descent direction out of $\widehat{\boldsymbol{\theta}}$. Therefore, we denote the reflection with respect to the plane Q by $R_Q : \mathbb{R}^3 \to \mathbb{R}^3$ which is given by $(x_1, x_2, x_3)^\mathsf{T} \mapsto (x_1, x_2, -x_3)^\mathsf{T}$. We choose an appropriate triangulation of B such that the corresponding $\mathbb{P}_1$-finite element space $\boldsymbol{V}_h$ satisfies

$$\boldsymbol{\zeta} \in \boldsymbol{V}_h \quad \Rightarrow \quad \boldsymbol{\zeta} \circ R_Q \in \boldsymbol{V}_h. \tag{6.3}$$

Clearly, a vector field $\boldsymbol{\theta} = (\theta_1, \theta_2, \theta_3)^\mathsf{T} : \mathbb{R}^3 \to \mathbb{R}^3$ is symmetric with respect to Q if

and only if

$$\boldsymbol{\theta} \circ R_Q(x) = (\theta_1(x), \theta_2(x), -\theta_3(x))^{\mathsf{T}} = DR_Q \boldsymbol{\theta}(x) \quad \forall x \in \mathbb{R}^3. \tag{6.4}$$

We define the vector field

$$\boldsymbol{\theta} := \widehat{\boldsymbol{\theta}} + DR_Q \widehat{\boldsymbol{\theta}} \circ R_Q$$

which is indeed symmetric with respect to Q. Due to $R_Q^{-1} = R_Q$ and $DR_Q^{-1} = DR_Q$, we readily obtain that (6.4) holds for $\boldsymbol{\theta}$ by calculating

$$\boldsymbol{\theta} \circ R_Q = \widehat{\boldsymbol{\theta}} \circ R_Q + DR_Q \widehat{\boldsymbol{\theta}} = DR_Q \boldsymbol{\theta}.$$

Next, we will prove that $\boldsymbol{\theta}$ also provides a descent direction. In fact, the bilinear form $\mathcal{B}$ that was used for our numerical experiments (6.2) consists of three summands. However, as the arguments are virtually the same for all of them, we will only focus on the first one, i.e.,

$$\widetilde{\mathcal{B}} : \boldsymbol{V}_h \times \boldsymbol{V}_h \to \mathbb{R}, \quad (\boldsymbol{\eta}, \boldsymbol{\zeta}) \mapsto \int_B D\boldsymbol{\eta} : D\boldsymbol{\zeta} \, dx.$$

Since $\widehat{\boldsymbol{\theta}} \in \boldsymbol{V}_h$, we have due to (6.3) that $\boldsymbol{\theta} \in \boldsymbol{V}_h$, and therefore

$$\begin{aligned} \widetilde{\mathcal{B}}(\widehat{\boldsymbol{\theta}}, \boldsymbol{\theta}) &= \int_B D\widehat{\boldsymbol{\theta}} : D(\widehat{\boldsymbol{\theta}} + DR_Q \widehat{\boldsymbol{\theta}} \circ R_Q) \, dx \\ &= \int_B D\widehat{\boldsymbol{\theta}} : [D\widehat{\boldsymbol{\theta}} + DR_Q D(\widehat{\boldsymbol{\theta}} \circ R_Q)] \, dx \\ &= \int_B D\widehat{\boldsymbol{\theta}} : [D\widehat{\boldsymbol{\theta}} + DR_Q (D\widehat{\boldsymbol{\theta}} \circ R_Q) DR_Q] \, dx. \end{aligned} \tag{6.5}$$

In order to exploit the symmetry properties of B, we introduce half-sets $B^+ = B \cap \{x_3 > 0\}$ and $B^- = B \cap \{x_3 < 0\}$. Thus, we may split the integral in (6.5) and apply the change of variables $x \mapsto R_Q(x)$ in the integral over B^-. Therefore, using the fact that $DR_Q = DR_Q^{-1} = DR_Q^{\mathsf{T}}$ we finally obtain

$$\begin{aligned} \widetilde{\mathcal{B}}(\widehat{\boldsymbol{\theta}}, \boldsymbol{\theta}) &= \int_{B^+} D\widehat{\boldsymbol{\theta}} : [D\widehat{\boldsymbol{\theta}} + DR_Q (D\widehat{\boldsymbol{\theta}} \circ R_Q) DR_Q] \, dx \\ &\quad + \int_{B^+} D\widehat{\boldsymbol{\theta}} \circ R_Q : [D\widehat{\boldsymbol{\theta}} \circ R_Q + DR_Q D\widehat{\boldsymbol{\theta}} DR_Q] \, dx \\ &= \int_{B^+} D\widehat{\boldsymbol{\theta}} : [D\widehat{\boldsymbol{\theta}} + DR_Q (D\widehat{\boldsymbol{\theta}} \circ R_Q) DR_Q] \, dx \\ &\quad + \int_{B^+} DR_Q (D\widehat{\boldsymbol{\theta}} \circ R_Q) DR_Q : [DR_Q (D\widehat{\boldsymbol{\theta}} \circ R_Q) DR_Q + D\widehat{\boldsymbol{\theta}}] \, dx \\ &= \int_{B^+} |D\widehat{\boldsymbol{\theta}} + DR_Q (D\widehat{\boldsymbol{\theta}} \circ R_Q) DR_Q|^2 \, dx > 0. \end{aligned}$$

Similar calculations yield $dJ_\gamma(\omega)(\boldsymbol{\theta}) = -\mathcal{B}(\widehat{\boldsymbol{\theta}}, \boldsymbol{\theta}) < 0$. Thus, $\boldsymbol{\theta}$ is a descent direction for J_γ that satisfies the symmetry property (6.4). Using $\boldsymbol{\theta}$ instead of $\widehat{\boldsymbol{\theta}}$ in our numerical algorithm yields an optimized design that is symmetric with respect to Q.

Finally, observe that if two symmetries with respect to two orthogonal planes Q_1 and Q_2 are desired, applying the symmetrization process described above first with respect to Q_1 and then with respect to Q_2 will yield the desired symmetries for $\boldsymbol{\theta}$.

REFERENCES

[1] G. Allaire, F. Jouve, and A.-M. Toader. Structural optimization using sensitivity analysis and a level-set method. *J. Comput. Phys.*, 194(1):363–393, 2004.

[2] V. Barbu and A. Friedman. Optimal design of domains with free-boundary problems. *SIAM Journal on Control and Optimization*, 29(3):623–637, 1991.

[3] J. W. Barrett and L. Prigozhin. Sandpiles and superconductors: nonconforming linear finite element approximations for mixed formulations of quasi-variational inequalities. *IMA J. Numer. Anal.*, 35(1):1–38, 2015.

[4] A. Bossavit. Numerical modelling of superconductors in three dimensions: a model and a finite element method. *IEEE Transactions on Magnetics*, 30(5):3363–3366, 1994.

[5] J. Céa. Conception optimale ou identification de formes: calcul rapide de la dérivée directionnelle de la fonction coût. *RAIRO Modél. Math. Anal. Numér.*, 20(3):371–402, 1986.

[6] J. De Los Reyes. Optimal control of a class of variational inequalities of the second kind. *SIAM Journal on Control and Optimization*, 49(4):1629–1658, 2011.

[7] M. Delfour and J. Zolésio. *Shapes and Geometries*. Society for Industrial and Applied Mathematics, second edition, 2011.

[8] Z. Denkowski and S. Migórski. Optimal shape design for elliptic hemivariational inequalities in nonlinear elasticity. In *Variational calculus, optimal control and applications*, volume 124 of *Internat. Ser. Numer. Math.*, pages 31–40. Birkhäuser, Basel, 1998.

[9] Z. Denkowski and S. Migórski. Optimal shape design problems for a class of systems described by hemivariational inequalities. *J. Global Optim.*, 12(1):37–59, 1998.

[10] C. M. Elliott and Y. Kashima. A finite-element analysis of critical-state models for type-II superconductivity in 3D. *IMA J. Numer. Anal.*, 27(2):293–331, 2007.

[11] G. Frémiot, W. Horn, A. Laurain, M. Rao, and J. Sokołowski. On the analysis of boundary value problems in nonsmooth domains. *Dissertationes Math.*, 462:149, 2009.

[12] B. Führ, V. Schulz, and K. Welker. Shape optimization for interface identification with obstacle problems. *Vietnam J. Math.*, 46(4):967–985, 2018.

[13] P. Fulmański, A. Laurain, J.-F. Scheid, and J. Sokołowski. A level set method in shape and topology optimization for variational inequalities. *Int. J. Appl. Math. Comput. Sci.*, 17(3):413–430, 2007.

[14] C. Heinemann and K. Sturm. Shape optimization for a class of semilinear variational inequalities with applications to damage models. *SIAM J. Math. Anal.*, 48(5):3579–3617, 2016.

[15] A. Henrot and M. Pierre. *Shape variation and optimization*, volume 28 of *EMS Tracts in Mathematics*. European Mathematical Society (EMS), Zürich, 2018.

[16] M. Hintermüller and A. Laurain. Optimal shape design subject to elliptic variational inequalities. *SIAM Journal on Control and Optimization*, 49(3):1015–1047, 2011.

[17] M. Hintermüller, A. Laurain, and I. Yousept. Shape sensitivities for an inverse problem in magnetic induction tomography based on the eddy current model. *Inverse Problems*, 31(6):065006, 25, 2015.

[18] K. Ito, K. Kunisch, and G. H. Peichl. Variational approach to shape derivatives. *ESAIM Control Optim. Calc. Var.*, 14(3):517–539, 2008.

[19] F. Jochmann. The semistatic limit for Maxwell's equations in an exterior domain. *Comm. Partial Differential Equations*, 23(11-12):2035–2076, 1998.

[20] H. Kasumba and K. Kunisch. On shape sensitivity analysis of the cost functional without shape sensitivity of the state variable. *Control Cybernet.*, 40(4):989–1017, 2011.

[21] M. Kočvara and J. V. Outrata. Shape optimization of elastoplastic bodies governed by variational inequalities. In *Boundary control and variation (Sophia Antipolis, 1992)*, volume 163 of *Lecture Notes in Pure and Appl. Math.*, pages 261–271. Dekker, New York, 1994.

[22] J. Kvitkovic, D. Davis, M. Zhang, and S. Pamidi. Magnetic shielding characteristics of second generation high temperature superconductors at variable temperatures obtained by cryogenic helium gas circulation. *IEEE Trans. Appl. Supercond.*, 25(3), 6 2015.

[23] A. Laurain. Analyzing smooth and singular domain perturbations in level set methods. *SIAM J. Math. Anal.*, 50(4):4327–4370, 2018.

[24] A. Laurain. A level set-based structural optimization code using fenics. *Structural and Multidisciplinary Optimization*, 58(3):1311–1334, Sep 2018.

[25] A. Laurain and K. Sturm. Distributed shape derivative *via* averaged adjoint method and applications. *ESAIM Math. Model. Numer. Anal.*, 50(4):1241–1267, 2016.

[26] J. L. Lions and G. Stampacchia. Variational inequalities. *Communications on Pure and Applied Mathematics*, 20(3):493–519, 1967.

[27] W. B. Liu and J. E. Rubio. Optimal shape design for systems governed by variational inequalities. I. Existence theory for the elliptic case. *JOTA*, 69(2):351–371, 1991.

[28] A. Logg, K.-A. Mardal, and G. N. Wells, editors. *Automated Solution of Differential Equations by the Finite Element Method*, volume 84 of *Lecture Notes in Computational Science and Engineering*. Springer, 2012.
[29] P. Monk. *Finite Element Methods for Maxwell's Equations*. Numerical Analysis and Scientic Computation. Clarendon Press, 2003.
[30] A. Myśliński. Domain optimization for unilateral problems by an embedding domain method. In *Shape optimization and optimal design (Cambridge, 1999)*, volume 216 of *Lecture Notes in Pure and Appl. Math.*, pages 355–370. Dekker, New York, 2001.
[31] J.-C. Nédélec. Mixed finite elements in $\mathbf{R}^3$. *Numer. Math.*, 35(3):315–341, 1980.
[32] P. Neittaanmäki, J. Sokołowski, and J. P. Zolesio. Optimization of the domain in elliptic variational inequalities. *Applied Mathematics and Optimization*, 18(1):85–98, Jul 1988.
[33] O. Pantz. Sensibilité de l'équation de la chaleur aux sauts de conductivité. *C. R. Math. Acad. Sci. Paris*, 341(5):333–337, 2005.
[34] L. Prigozhin. On the Bean critical-state model in superconductivity. *European J. Appl. Math.*, 7(3):237–247, 1996.
[35] L. Qi. Transposes, L-eigenvalues and invariants of third order tensors, 2017.
[36] T. Roubícek. *Nonlinear Partial Differential Equations with Applications*. International Series of Numerical Mathematics. Springer Basel, 2013.
[37] J. Sokołowski and A. Żochowski. Modelling of topological derivatives for contact problems. *Numer. Math.*, 102(1):145–179, 2005.
[38] J. Sokołowski and J.-P. Zolésio. *Introduction to shape optimization*, volume 16 of *Springer Series in Computational Mathematics*. Springer-Verlag, Berlin, 1992.
[39] K. Sturm. Minimax Lagrangian approach to the differentiability of nonlinear PDE constrained shape functions without saddle point assumption. *SICON*, 53(4):2017–2039, 2015.
[40] R. Trémolières, J. L. Lions, and R. Glowinski. *Numerical Analysis of Variational Inequalities*. Studies in Mathematics and its Applications. Elsevier Science, 1981.
[41] F. Tröltzsch and I. Yousept. PDE-constrained optimization of time-dependent 3D electromagnetic induction heating by alternating voltages. *ESAIM Math. Model. Numer. Anal.*, 46(4):709–729, 2012.
[42] M. Winckler and I. Yousept. Fully discrete scheme for Bean's critical-state model with temperature effects in superconductivity. To appear, SIAM J. Numer. Anal., 8 2019.
[43] I. Yousept. Hyperbolic Maxwell variational inequalities of the second kind. *ESAIM: COCV*. DOI: 10.1051/cocv/2019015.
[44] I. Yousept. Optimal control of Maxwell's equations with regularized state constraints. *Computational Optimization and Applications*, 52(2):559–581, 2012.
[45] I. Yousept. Optimal Control of Quasilinear $\boldsymbol{H}(\mathbf{curl})$-Elliptic Partial Differential Equations in Magnetostatic Field Problems. *SIAM J. Control Optim.*, 51(5):3624–3651, 2013.
[46] I. Yousept. Hyperbolic Maxwell variational inequalities for Bean's critical-state model in type-II superconductivity. *SIAM J. Numer. Anal.*, 55(5):2444–2464, 2017.
[47] I. Yousept. Optimal control of non-smooth hyperbolic evolution Maxwell equations in type-II superconductivity. *SIAM J. Control Optim.*, 55(4):2305–2332, 2017.